University of Missouri – Chemistry

Radiochemical and Analytical Methods of Analysis of Radiological Dispersal Devices

A Dissertation Presented to the Graduate School of the University of Missouri-Columbia

In Partial Fulfillment of the Requirements for the Degree of
Doctor of Philosophy

by

Simmonds, Isaac D. (MU-Student)

Dr. J. David Robertson, Dissertation Supervisor

May 2015

The undersigned, appointed by the Dean of the Graduate School, have examined the dissertation entitled:

Radiochemical and Analytical Methods of Analysis of Radiological Dispersal Devices

Presented by Isaac D. Simmonds
A candidate for the degree of Doctor of Chemistry
And hereby certify that in their opinion it is worthy of acceptance.

_____
Professor J. David Robertson
Committee Head

_____
Professor Michael Greenlief
Department of Chemistry

_____
Professor Gary Baker
Department of Chemistry

_____
Professor Mark Lee
Department of Chemistry

_____
Professor John Brockman
Missouri University Research Reactor

I would like to thank all of my family and friends who have supported and stood by me through some of the hardest and most rewarding years of my life as I have pursued this degree. A very special thanks goes to my wonderful wife Krystal who has stood by my side and has been all the support that I needed to continue on in school. She has also been the perfect reason to take the time outside of work to spend life with. Thanks also to my sons Jaden and Luke who bring so much joy to my life. Thank you to my dad and my grandfathers who taught me that; “hard work is good for you” and the joy of science and discovery. Thank you to my mom, my siblings, my grandmothers, and extended family who have all been the source of so much support, encouragement and strength for my entire life.

For since the creation of the world God’s
invisible qualities—his eternal power and
divine nature—have been clearly seen, being
understood from what has been made, so
that people are without excuse.
–Romans 1:20

Acknowledgements

This work could not have been accomplished without the knowledge, technical support, encouragement and funding from many individuals, groups, and agencies to whom I am very grateful.

The funding of this work has been supported by multiple agencies. The work involving the analysis of iridium as well as the funding of my salary for a large portion of my graduate career was funded by the Department of Homeland Security, Department of Nuclear Detection Office through Savannah River National Laboratory. Special thanks goes to Donna Beals, Jacob Venzie, and their colleagues at Savannah River for providing me the opportunity to work on this project and for their support and guidance for the project. Also thanks goes to Martha Finck and her colleagues at Idaho National Lab for picking up the project and providing technical advice and the activated iridium samples helping the project to completion. Enriched iridium targets were provided courtesy of QSA Global Inc. and Dr. Mark Shilton.

There were also many individuals who provided technical and research guidance in the building and use of various equipment and instruments that are described in this thesis. Dr. Alan Ketring was the point of contact for the iridium work and also provided technical advice and guidance for the project. Mr. Jim Guthrie and John Brown of MURR introduced me to and trained me on all of the ICP-MS instruments that were used for this work. Jim also provided much guidance and knowledge for the development and method of analysis using the instruments and sample preparation. Mr. Bill Vellma of the University of Missouri Chemistry Department provided technical abilities in developing and building the electrochemical cell that is described. Mr. Scott Cadell of MURR

provided information and training of MURR's neutron activation analysis system and also spent much time shooting rabbits and counting samples with me.

I also owe a great deal of thanks to the Robertson research group at the University of Missouri's Chemistry Department. The members provide a lot of support and advice as well as listening to many hours of presentations and practice speeches. Mark McLaughlin is owed much thanks for his help in learning the synthesis and technical knowledge of the nanoparticles. Tom Brossard did much work with the design and use of the electrochemical cells. Logan Sutherlin provided much help in nanoparticle synthesis and NAA runs.

Table of Contents:

Chapters:

List of Acronyms:

Neutron Activation Analysis.....NAA

Instrumental Neutron Activation Analysis .....INAA

Inductively Coupled Plasma – Mass Spectrometry ..... ICP-MS

Inductively Coupled Plasma – Quadrupole Mass Spectrometry ..... ICP-QMS

Inductively Coupled Plasma – Sector Field Mass Spectrometry.....ICP-SFMS

Radiological Dispersal Device..... RDD

Department of Homeland Security .....DHS

Department of Defense .....DOD

X-Ray Fluorescence.....XRF

High Pressure Liquid Chromatography ..... HLPC

Mass Spectrometry.....MS

Time of Flight Mass Spectrometry .....TOF-MS

Thermal Ionization Mass Spectrometry..... TIMS

International Atomic Energy Association.....IAEA

Special Nuclear Material.....SNM

Kinetic Energy Discrimination ..... KED

Platinum Group Metal.....PGM

Alternating Current .....AC

Direct Current .....DC

Poly Ether Ether Keytone .....PEEK

Variable AC ..... VARIAC

Relative Standard Deviation .....RSD

Alfa Aesar ..... AE

Alfa Omega Samples .....AOS

Principle Component .....PC

Principle Component Analysis .....PCA

Standard Deviation.....STDEV

High Flux Reactor.....HFR

Nuclear forensics ..... NF

Ammonium Nitrate in Fuel Oils .....ANFO

Tri Nitro Tolulene.....TNT

Penta-Erythritol Tetra-Nitrate .....PETN

octahydro-1,3,5,7-tetranitro-1,3,5,7-tetrazocine ..... HMX

Improvises Explosive Device .....IED

Home-Made Device..... HMD

Plastic Bonded Explosives.....PBD

Victim-Operated Improvised Explosive Device ..... VOIED

Command Operated Improvised Explosive Devices ..... COIED

Office of Technology Assessment..... OTA

High Flux Reactor.....HFR

National Rifle Association..... NRA

National Mining Association..... NMA

Radiofrequency Identification ..... RFID

X-Ray Diffraction ..... XRD

Transmission Electron Microscopy ..... TEM

Electron Energy Loss Spectroscopy ..... EELS

Missouri University Research Reactor ..... MURR

Highly Enriched Uranium ..... HEU

High Purity Germanium ..... HPGe

National Mining Association ..... NMA

Deuterium-Deuterium ..... D-D

Deuterium-Tritium ..... D-T

Tri-Poly Phosphate ..... TPP

List of Figures:

List of Tables:

List of Equations:

Abstract

The events on September 11th 2001 and subsequent attacks in America and around the world have brought a renewed interest in the nation's security including the concern over the use of a nuclear or a radiological dispersal device (RDD). Research utilizing NAA and ICP-MS has been done in two separate projects in order to help address some of these concerns. A research assistantship from Savannah River National Laboratory was granted in order to identify the impurities and isotope ratios of ^{192}Ir sources (chapters 2-4). An electrochemical dissolution method of the iridium was developed and used for sample preparation for ICP-MS analysis. ICP-MS analysis was then used to identify and quantify impurities and isotope ratios in iridium from various sources. The second research project has developed a series of lanthanide phosphate based nanoparticles for use as tagging and tracking agents (chapters 5-7). The composition of the nanoparticles were varied to provide a unique signature that can be rapidly and precisely measured in the field via neutron activation analysis. The nanoparticles could be used as a real-time in the field method for tracking and identifying materials such as explosives in a post detonation scenario.

Chapter 1

Overview

Introduction 1.1

The events on September 11th 2001 and subsequent attacks have brought a renewed interest in the nation's security including the concern over the use of a nuclear or a radiological dispersal device (RDD). There is concern over such devices because there are an estimated 100,000 "orphaned" radioactive sources around the globe and were over 300 reported cases of attempted smuggling of nuclear material between 1995 and 2005 [1-2]. Given that an attack using a nuclear or radiological device is quite possible, there is a need to track radioactive materials and identify the source of materials used in a RDD.

Nuclear Forensics can be defined as "the technical means by which nuclear materials, whether intercepted intact or retrieved from post-explosion debris, are characterized (as to composition, physical condition, age, provenance, history) and interpreted (as to provenance, industrial history, and implications for nuclear device design)." [1].

Nuclear Devices and Forensic Response 1.2

Nuclear forensic analysis encompasses three scenarios where different possible types of materials/devices are used. The first and most dangerous scenario is the detonation of an actual nuclear weapon which is greater than 1 kiloton [3]. A scenario in which an individual, a group of individuals, or a rogue nation obtains and detonates such a device in a populated area is by far the worst possible case that could result in tens or hundreds of thousands of casualties. A second scenario involves the use of some fissile

material in a detonated device [3]. Such a device would still cause a large amount of damage and contaminate an area of several city blocks. It would also most likely cause many casualties but would not reach the scale of a true nuclear weapon. A third scenario involves the use of a traditional explosive device with high explosives and radiological materials contained within the device. Such a device is called a Radiological Dispersal Device (RDD) or is more commonly known as a dirty bomb [1]. The material in such a device would cause less damage than the other two scenarios but could still destroy a building or public area from the detonation of the explosive material causing many casualties and spread radiological contamination over a small area. The potential radiological exposure would be life-threatening to very few if any people however, use of the radiological material could cause large spread panic and result in deaths and injuries due to the public's reaction to the device. Emergency response times to such an event due to added administrative controls or fear of first responders could also lead to individuals with injuries at the site not receiving care that is urgently needed.

In order to be able to respond to such an event and identify the materials and the parties responsible requires; knowledge of the potential types of devices and materials that could be used, development of databases with information on signatures also known as "fingerprints" which are special characteristic identifiers of materials and devices, and the development of a method for quick and accurate analysis of the materials [3]. Knowledge of potential devices that could be used would come from individuals with experience working in the nuclear science and engineering fields with knowledge of nuclear devices and materials. It is also important to work with the military, intelligence, and law enforcement fields in order to obtain information on the types of devices that

have commonly been found or used in the past. Method development and the creation of databases of nuclear materials requires technical expertise for the analysis of nuclear materials. It also requires a focused and well planned vision for the type of information needed in order to have the appropriate response to nuclear event.

Radiochemical and Analytical Techniques 1.3

There are a variety of radiochemical and analytical techniques that are effective methods of analysis of materials at minor and trace levels that could serve as a means of identification. Radiochemical techniques include destructive and non-destructive forms of analysis. Radiochemical techniques are useful for identifying and dating materials where the emitted radiation from the source is measured by alpha, beta and gamma spectroscopy. Other methods include using an emitted particle or photon to interrogate a sample. These techniques include NAA (Neutron Activation Analysis) and XRF (X-Ray Florescence) [4-6]. Various other organic and inorganic radiochemical methods and techniques could also be useful for the analysis of radioactive and nuclear materials.

Common analytical techniques that can be used for analysis of samples include; mass spectrometry (MS), High Pressure Liquid Chromatography (HPLC) coupled with methods of analysis such as mass spectroscopy, and various absorption and luminescence spectroscopies. Mass spectrometry is becoming the most widely used analytical method in nuclear forensics. Various mass spectrometry techniques are used including; Inductively Coupled – Mass Spectrometry (ICP-MS), Time of Flight Mass Spectrometry (TOF-MS), and Thermal Ionization Mass Spectrometry (TIMS). All of these techniques have characteristic advantages and disadvantages to their use [7].

Having strong radiochemical and analytical methods for analysis and quantification of nuclear forensic materials is vital for providing quality information to the appropriate authorities for attribution of the material and for a strong deterrent to those who may attempt future attacks.

Forensic Analysis 1.4

As stated before it is important that forensic personnel are able to characterize nuclear samples as to their composition, physical condition, age, provenance, and history [2]. There are many characteristics that can be measured and analyzed in order to provide information on the source of the radiological material.

One important measurement is of the isotope ratios. Isotope ratios can provide information on whether the material had been enriched, the type and length of irradiation, as well as the age or time that the material has been decaying [8-9]. Another important measurement is the analysis of the minor and trace impurities in a sample. The impurities can give information on the location the material was originally mined, what chemicals were used in the separations and purification process and where the source has been recently [9-10]. All of the physical properties listed above can then be collected and be used in the forensic investigation to identify those responsible.

Project Overview 1.5

The objective of this project is to use radiochemical and analytical techniques to analyze materials that have the potential to be used in an RDD. Methods and procedures have been developed for the effective tagging and tracking of plastics such as explosives with lanthanide nanoparticles. The identification of the nanoparticles in the field will be

done with NAA using a portable neutron source and gamma spectrometer. A method for the dissolution and analysis of ^{192}Ir sources with ICP-MS has also been developed.

Chapter 2

Nuclear Forensic Attribution

Introduction 2.1

The United States Federal Government as well as the International Atomic Energy Agency (IAEA) have invested a great deal of time and effort in developing an international database which contains information to help track and identify radioactive sources [1,2]. This database includes everything from manufacturer information, to types of devices and processes that sources are used for, and chemical/physical characteristics of the material. When nuclear/radiological materials are found or used in an attack, the process of identifying what happened, where it happened, and how it was accomplished can be referred to as attribution. A more thorough explanation is detailed as; "nuclear attribution integrates all relevant forms of information about a nuclear smuggling incident into data that can be readily analyzed and interpreted, and that will then form the basis of a confident and meaningful response to the incident [3]."

In order to identify the origin of a material and how it could have been obtained for use in a nuclear or radiological device, there are a variety of physical, chemical, and nuclear properties that can be used to help attribute what types of materials were used. Material attribution along with information obtained through law enforcement and government intelligence agencies is brought together to create the best possible scenario of what happened and find those responsible in such an event so that a plan can be devised with the most appropriate response.

Nuclear forensics attribution is relevant in cases for both Special Nuclear Material (SNM) and Radiological Dispersal Device (RDD) scenarios. Understanding these

materials and finding better ways to track them is of great importance to ensure the most effective attribution program. This chapter discusses attribution of radiological materials.

Methods of Analysis 2.2

There are a variety of radiochemical and analytical techniques used for the analysis of radiological materials. There are a few characteristics that the analysis methods must contain to make them the appropriate method of. In the analysis of archaeometric samples, Janssens offer several factors which need to be taken into account when selecting a method of analysis for the attribution of a material. These factors include: sensitivity, accuracy, precision, destructive or non-destructive, surface or bulk analysis, laboratory or in-field analysis and appropriateness for the type of sample. Janssens et al. cited the six most important characteristics of a method for analyzing materials as the following: versatile, non-destructive, fast, universal, sensitive, and multi-elemental [12-14].

Taking into consideration all of the previously mentioned parameters for selecting a sample analysis method, the chosen analysis method for radiological sources must contain the following abilities. The sample analysis method must be able to quantify complex matrices at varying concentrations within the sample matrix. Other important factors include; the ability to perform isotopic analysis, the ability to do analysis in a hotcell, the ability to be able to analyze a sample which could be in various physical forms (powder, seed, disk, etc.), the ability to perform the analysis with limited sample material, and the ability to perform the analysis quickly.

ICP-MS and INAA/gamma spectroscopy are complimentary methods which are both used for the analysis of trace elements in a sample matrix at low concentrations.

While ICP-MS is a growing field which is replacing the use of INAA in many areas, INAA still provides unique capabilities that make it a useful technique for many applications [4]. Table 2.1 [5] summarizes the advantages of each technique and table 2.2 [5] summarizes each techniques disadvantages.

INAA	Small sample size $<10^{-6}$ grams	High accuracy ~1%	Simple Sample preparation	Independent of sample chemical state	non-destructive
ICP-MS	Low detection limits $<10^{-6}$ grams	High accuracy ~1%		Can be connected to chemical separation techniques (LC, GC, etc.)	Isotopic analysis possible

Table 2.1: The advantages of ICP-MS and INAA as multi-element analysis techniques.

As can be seen, INAA and ICP-MS have similar detection limits for many elements, especially the transition and lanthanide metals, with a high level of accuracy and precision. INAA has the advantages of performing non-destructive analysis of select samples with little to no sample preparation. While ICP-MS typically requires sample preparation, it can provide isotopic information which typically is not possible with INAA.

INAA	Can be susceptible to matrix interferences	May leave sample activated for extended periods of time	Requires access to high neutron flux source	Requires sample with large cross sections for quick analysis
ICP-MS	Requires sample preparation	Is a destructive method	Cannot be done in-field	

Table 2.2: The disadvantages of ICP-MS and INAA for multi-elemental analysis.

Another important factor in choosing between these methods is that to reach the lowest detection limits of INAA a high flux of neutrons on the order of ca. 1×10^{14} $n*cm^{-2}*s^{-1}$ is needed to activate the material enough with sufficient gamma emissions for good

counting statistics. ICP-MS instruments are more readily available and cost effective for most laboratories. A drawback to ICP-MS is that there is currently no in-field ICP-MS capable of making such measurements while INAA can be done in-field within certain limitations.

ICP-MS Instrumentation 2.3

ICP-MS instrumentation is one of the most commonly used methods for nuclear forensic analysis of radiological samples [7]. It is widely used because it can be used for both trace metal and isotopic analysis of simple or complex matrices. All liquid sample introduction ICP-MS systems contain four main stages; a sample introduction system which nebulizes liquid samples into an aerosol, an argon plasma which vaporizes and ionizes the sample, the mass separator, and the detection system. Samples may be analyzed in the solid form through laser ablation but this approach does not provide the accuracy and precision obtained with liquid sample introduction.

The instruments applicable to this project introduce liquid samples into the system either manually or with an auto sampler both of which utilize a pump that transfers the liquid sample to be nebulized, in this work, at a rate of ~1mL/min. The systems allow for manual changing of the amount of sample introduced at rates from microliters to milliliters per minute dependent upon the concentration and amount of sample matrix being analyzed. In this work, the liquid sample is nebulized with a PFA (perfluoroalkoxyethylene) polymer micro-concentric nebulizer which converts the solution into an aerosol for atomization and ionization of the analytes before introduction to the quartz jacketed spray chamber. The spray chamber reduces the aerosol droplet size in order to minimize matrix effects. The sample in aerosol form is then introduced into

the plasma. The plasma is sustained by a water-cooled, copper radio frequency generator which is generated initially by a high voltage spark which ionizes the argon gas. Argon gas travels through a quartz tube contained within the copper coil at a rate of around 15 L/min. The magnetic field produced by the copper coil sustains the plasma. The plasma reaches electron temperatures around 10,000 degrees K. The plasma vaporizes, atomizes, and ionizes the aerosol introduced to the plasma. The resulting ions then travel through a series of sample and skimmer cones. These cones collimate the beam and provide the interface between the outside of the instrument at atmospheric pressure and the inner chamber where vacuum pumps reduce the pressure to ca. 10^{-6} torr. The positively charged ions produced in the plasma are then separated by their mass to charge ratio. There are many different types of mass separators which include quadrupoles, octapoles, and curved magnetic sectors. Ions with the selected mass to charge ratio are then measured using either a dynode detector or faraday cup. In either case the ions produce an electrical signal and individual events are relayed to counts and output into the computer software. In this work both a high resolution instrument produced by AXIOM and a quadrupole produced by NEXION were used for sample analysis. A description of the instruments and their use for nuclear forensic analysis is provided below.

Sector Field High Resolution ICP-MS

A schematic of the A VG Axiom ICP-Sector Field Mass Spectrometer (ICP-SFMS) from Thermo Scientific (Waltham, MA, USA) is given in figure 2.1

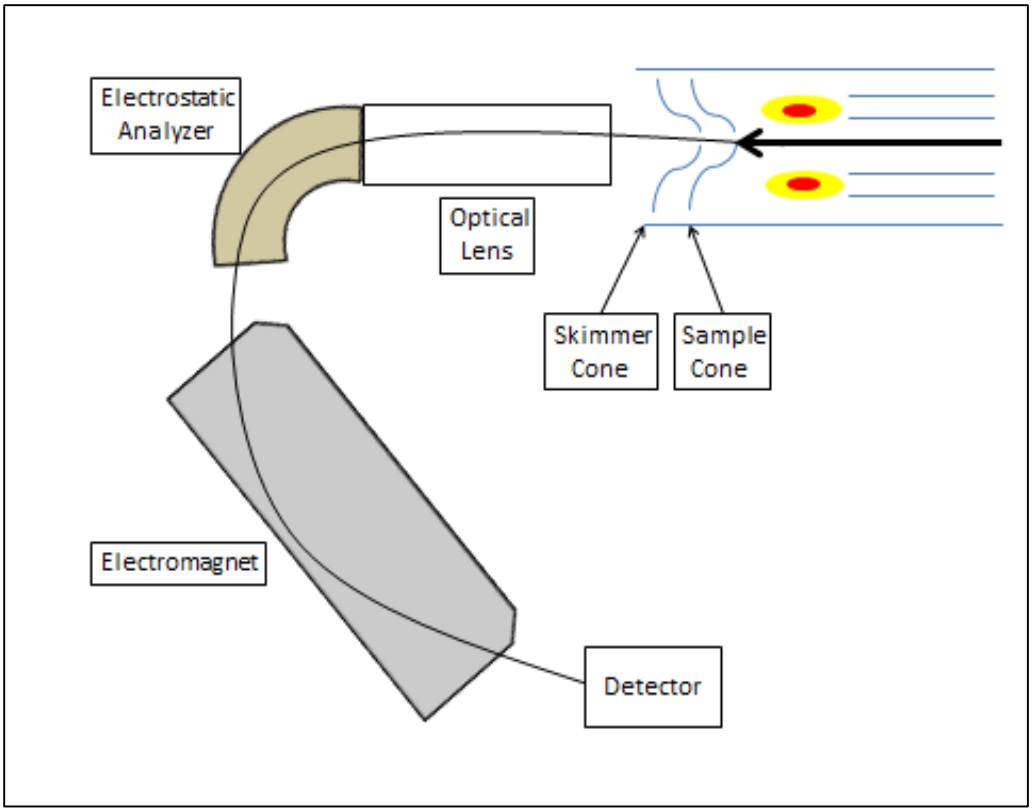

Figure 2.1: A schematic of the VG Axiom High Resolution – Sector Field - ICP-MS.

High resolution ICP-SFMS is used when peaks have similar mass to charge ratios and separation of the signals from two or more peaks is needed that cannot be effectively distinguished by other ICP-MS instruments. This is important because interferences can affect the accuracy in the quantification of analytes in a given sample. With higher mass to charge separation the instrument is able to ensure that the signal is due to the element of interest and that there is not a polyatomic or isobaric interference produced in the plasma or from other materials in the sample matrix.

High Resolution Instrumentation

The VG axiom instrument has several advantages for analyzing samples. This particular instruments (along with many other high resolution instruments) peak resolution can be varied in order to balance the achievement of good peak separation,

analysis speed, and measurement sensitivity. The resolving power is a term defined by the variable R; R = m/(|m1-m2|), where m1 is the mass of one species or isotope and m2 is the mass of the species or isotope it must be separated from, and m is their nominal mass. Many elements of interest have potential polyatomic interferences. Table 2.3 lists some of the most common interferences which need to be separated with a high resolution instrument [15].

Analyte	Interference	|Δ m|	m	R
$^{75}As = 74.92160$	$^{40}Ar^{35}Cl = 74.93123$	0.00963	75	7788
$^{52}Cr = 52.94065$	$^{37}Cl^{16}O = 52.96081$	0.02016	53	2629
$^{56}Fe = 55.93494$	$^{40}Ar^{16}O = 55.95729$	0.02235	56	2505
$^{40}Ca = 39.96259$	$^{40}Ar = 39.96238$	0.00021	40	190476

Table 2.3: Analytes which have potential chloride or oxide polyatomic interferences in an argon plasma with the resolving (R) values needed to effectively separate the interferences. (table adapted from USGS ICPMS laboratory [15])

The greater the peak resolution needed, the longer time that is needed to obtain enough counts for acceptable counting statistics. High resolution instruments with variable resolving powers are able to achieve varying resolutions by adjusting the width of the entrance and exit slits. Narrowing the slit width increases peak resolution by being more selective in the ions that are allowed to pass through the slits to the detector. This leads to sensitivity (signal intensity) being sacrificed due to the greater number of ions which are selectively prevented from passing through the slits. A typical quadrupole instrument has a resolving power (R) of 300 or less. The Axiom has peak resolving powers ranging from 300 to 10,000.

The system also has a high ion transport efficiency creating a better sensitivity for most elements. The VG Axiom has a design which limits the number of photons from the plasma that can make it all the way through the instrument to the detector which reduces the amount of noise in the system. The combination of low noise and high ion transport efficiency produces low detection limits for the system.

Quadrupole ICP-MS

A quadrupole ICP-MS (ICP-QMS) was also used in this work. ICP-QMS is useful for fast analysis of inorganic samples at high sensitivities. Quadrupole instruments are also more prevalent in laboratories making the instrument more readily available for use in the event fast sample analysis turn-around is needed. Because of its smaller footprint, it is also the type of instrument that would likely be installed in a hot cell for high activity samples analysis. Sample impurities and isotope ratios that are measured on the high resolution instrument can also be measured with the quadrupole instrument assuming that there is sufficient mass separation.

Quadrupole Instrumentation

The NEXION 300S quadrupole ICP-MS instrument, seen in figure 2.2, was used for the analysis of the majority of the samples analyzed in this project. Some unique features of the NEXION 300S are that it has three skimmer cones as well as three quadrupoles. The three cones, known as the triple cone interface are used to help increase the amount of collimation (lower divergance) of the ion beam as well as helping achieve a better vacuum for the interal chamber of the instument. This leads to greater sensitivity and stability of the signal. The three quadrupoles of the instrument are used for deflecting uncharged species and selecting the desired mass to be measured at the detector. The first

of the three quadrupoles, known as the ion deflector as seen in figure 2.2, turns the beam of charged particles 90 degrees from its original path effectively separating out any uncharged species in the beam. The second quadrupole is used for the selection of the desired mass to charge ratio inside the collision cell to be analyzed. The third quadrupole after the collision cell further selects and collimates the mass to charge ratio to be measured at the detector. The use of two quadrupoles for mass to charge selection increases the sensitivity and decreases the amount of interferent masses reaching the detector.

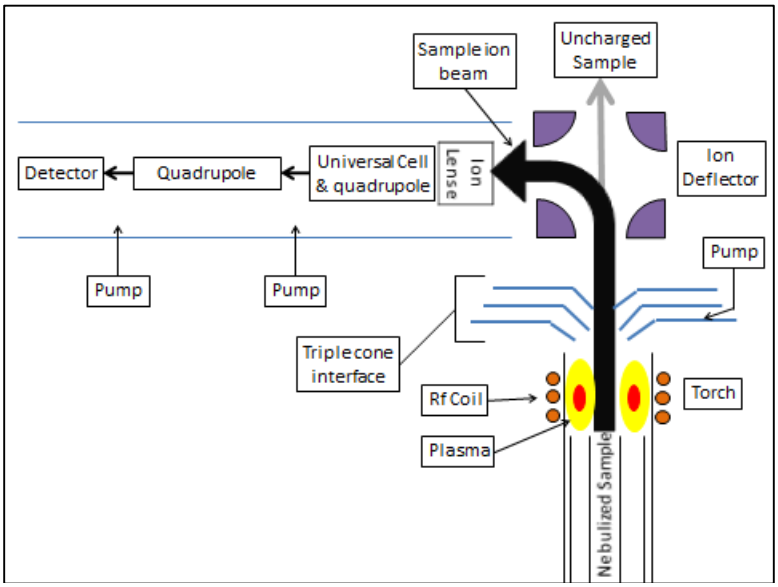

Figure 2.2: Schematic of NEXION 300S quadrupole ICP-QMS instrument.

The quadrupole is used to select a specific mass to charge ratio to be measured by utilizing the fast switching between positive and negative electric potential changes in its four poles. To begin, the top and bottom poles have a positive charge while the two side poles have a negative charge. This attracts all of the positively charged ions to the horizontal plane due to the negatively charged poles. The charge is then reversed in all four poles with the top and bottom poles containing the negative charge and the side poles containing the positive charge. This leads to the ions in the beam to move towards

the verticle plane. With a rapid simultaneous alternation of the poles from positive to negative, the ions in the beam will begin to move through the quadrupole. Due to the alternation of the electric fields, the ions in the beam with too high or too low of a charge to mass ratio will be expelled from the beam due to unstable trajectories leaving only the pre-selected ions with the correct mass to charge ratio to pass completely through the qudarupole.

There are three possible modes in which the NEXION can be operated (table 2.4). The system has a collision cell which can be run in standard, collision mode with kinetic energy discriminator, and reaction mode. The collision cell in standard mode leaves the cell under vacuum allowing the ion beam to pass through unhindered. The kinetic energy discriminator (KED) introduces a non-reactive-gas such as helium to the cell chamber. The neutral helium atoms collides with the introduced sample ion beam. This is mostly used for the removal of diatomic interferences since they have a much higher probability of changing the flight path through interaction with the He while allowing the monoatomic charged particles through at a higher rate. The KED mode does, however, reduce the sensitivity of the entire measurement. This approach has the added advantage when a sample needs to be measured at a higher concentration when either liquid dilution is not practical or has the potential to introduce a new interferant. In the reaction mode, much like KED mode, a gas is introduced into the collision cell but in this case it is a reactive gas. This leads to the reactive gas reacting in a predictable fashion with either the inferences or even the element of interest in the sample matrix to generate a molecular species whose mass is either measured (analyte) or discriminated (interference).

	Standard Mode	Collision Mode (KED)	Reaction Mode
How it works	Collision cell gas is turned off and works as though there is no cell. This provides the best possible detection limits provided that there is no required interference correction.	A non-reactive gas is introduced into the cell to collide with interfering ions with larger diameters and polyatomic species, reducing their kinetic energy so they may be removed through kinetic energy discrimination.	A highly reactive gas (or gasses) is introduced in to the cell to create predictable reactions. Any side reactions and resulting new interferences are instantly removed by a scanning quadrupole so only the element of interest is passed to the analyzing quadrupole and detector.
Possible uses	Routine applications requiring high throughput that have few interferences.	Applications that may be susceptible to interferences, or analyses where you simply want to remove any unknown interferences making it useful for environmental testing or samples with unknown interferences.	Applications demanding a high level of interference removal.
Collision cell gas	None	non-reactive (helium)	reactive (methane or oxygen)

Table 2.4: Various properties and common uses of the collision cell used in the NEXION ICP-MS 300S (Table adapted from NEXION ICPMS Manual [16].

Radiological Sources 2.4

Radiological sources are classified differently from special nuclear material. SNM is a material that is capable of nuclear detonation through fission or fusion (or used in the design of a nuclear weapon). SNM includes highly enriched U-233, U-235, and all Pu isotopes [3]. Radiological sources are used for a wide variety of purposes therefore a large number of different isotopes are used for their unique properties. These important varying properties include; half-life, type of emitted radiation, energy of radiation and chemical morphology. The most commonly used industrial sources are Co-60, Cs-137, Sr-90 and Ir-192. [102] These sources are the most common because they have half-lives on the order of days to a few years which makes them useful for a long period of time but

they will decay over the course of a short enough period of time making the long term disposal less hazardous and therefore less complicated. They are also widely used because they are all beta and gamma emitters which lends them to a wide variety of applications.

Sealed Sources

Sealed sources are a particular type of radiological source. A concern when making a radiological source is the potential for the source to degrade creating a dispersal risk. In order to avoid dispersal or contamination one of two things must be done so that the material does not change chemically over its lifetime. The first method is to choose a chemically inert material. Examples of chemically resistant sources are iridium sources. Iridium is very resistant to redox reactions and is a hard metal with a high boiling point. Therefore iridium sources can be used with little concern for source corrosion or contamination problems. The number of elements that have such favorable chemistry however is greatly limited. There are a number of other elements that have great nuclear properties for a radiological source but are much less resistant to redox reactions or come in powdered form. One such example is Cs sources. Cesium sources are usually in the form of salts which often are in powder or crystalline form. The powders could easily spread causing contamination of personnel and equipment. A sealed source is the method used to avoid this problem. The activated Cs salt which is in powder or crystal form, is placed into a small metal vial and then welded or soldered shut [2].

Iridium-192 Sources

Iridium-192 sources are one of the 4 most used radiological sources around the world [2]. Iridium-192 is used for a wide variety of purposes. It has a half-life of 73.83

days making it useful for a reasonable period but does decay over the course of a few years so that long term storage is not a concern. It emits beta particles at maximum energies of 538 and 635 keV and gamma rays at energies of 316 and 468 keV making it useful for both non-destructive imaging as well as medical purposes. As stated above it is chemically inert making the source very stable. The iridium sources are made by irradiating iridium in the neutron rich environment of a nuclear reactor for a time period on the order of several weeks to a little over a month. Because natural iridium has two stable isotopes ^{191}Ir (37.3%) and ^{193}Ir (62.7%), both ^{192}Ir and ^{194}Ir are produced. The presence of ^{194}Ir is not problematic with the radiography sources with the extra activity even being helpful in the imaging process. The extra gammas do however pose a problem with the medical sources with unwanted exposure to the patient. In the case of medical sources, the iridium is enriched in ^{191}Ir to above 80% enrichment. There is no enrichment needed for the radiography source so natural iridium is used.

Ir-192 sources are used for a variety of purposes in both public and private industry. One of the most common uses of these sources is for brachytherapy treatment of cancer. The low energy beta particles as well as the 74 day half-life are ideal for this form of treatment. Small “seeds” weighing approximately 5 mg with activities of up to 100 Ci are inserted into the tumor and provide a constant long term irradiation of the tumor and surrounding tissue [17-18].

Iridiuim-192 sources are also often used for non-destructive imaging sources because of its two strong gamma rays. The half-life once again is ideal for these applications. The radiography sources come in the shape of disks weighing approximately 20 mg and are

activated to activities ranging from 5 to150 Ci each. As many as 12 disks can be packaged together to make a higher activity source [19].

Figure 2.3: Medical iridium "seeds" which are implanted for brachytherapy treatments.

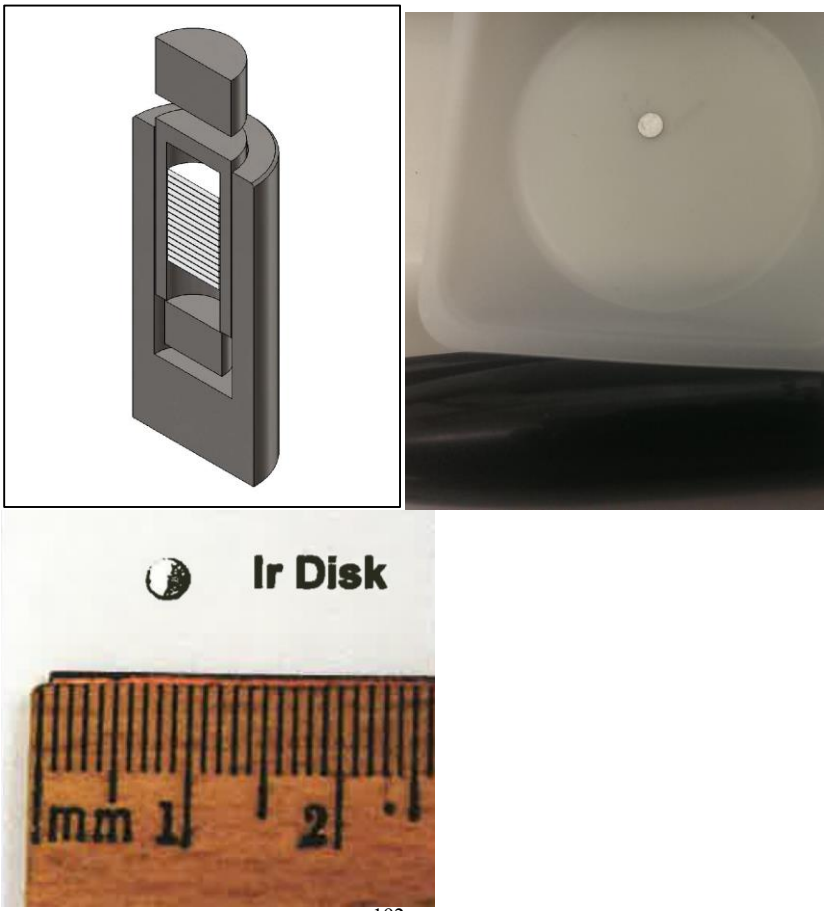

Figure 2.4: Cross section of ^{192}Ir disks encapsulated in in source for radiography and individual disk.

Trace Impurity Analysis 2.5

One of the best ways to attribute where a material may have originated is through the identification and quantification of its trace impurities [2, 7-10]. If the source material were to be mined in several different locations around the globe, each mined sample could have its own characteristic signatures or "fingerprint" of trace impurities that remained through the purification process. Identifying the trace impurities in a sample and quantifying the amount of each of those impurities can help in confirming or excluding the possible original source of a material. There are also a variety of separations processes that are used in the purification process of materials which in many cases is very complex and requires the use of various acids, reagents, and separations methods. The separation process can therefore fractionate the trace impurities in the material or introduce new impurities that can be measured and possibly used for attribution as well.

Natural Ores & Mining Processes

It is rare for a material to be mined in its pure chemical form. Most often ores are mined which contain multiple elements of similar chemical reactivity. For instance, "natural PGM (Platinum Group Metal) deposits are almost always related to basic igneous rocks and are closely associated with copper, nickel and iron sulfides [17, 20]." The PGM's only compose a small portion of the bulk ore that is mined. The PGM's are actually considered byproducts and separated out from copper, iron or nickel. With the growing number of uses for rare earth and platinum group metals, these byproducts are separated out individually and used for a variety of purposes.

Iridium is very resistant to attack from even the strongest acids. Ore's containing iridium often have other platinum group metals (PGM's) including; platinum, rhodium, ruthenium, tungsten, osmium, silver, tantalum, and gold [21]. Many of these elements have similar chemistry in the +3 and +4 oxidation states. Because of this, there is a complicated process for the separation of iridium from its natural ore.

Chemical Separation Process

Once an ore has been mined, the desired materials must be separated from the bulk material. There are various separations processes that may be involved in separations depending on the type of element to be extracted, the types of impurities, and the cost and practicality of the applicable separation methods.

There are two different methods for separating iridium from other platinum group metals found in common iridium containing ores. The first of the two methods also known as the more classical method is an organic separations method outlined in Appendix A. This method uses various organic reagents most of which are acids to dissolve and change the oxidation states of the materials to eventually separate out iridium. The second method known as the modern method utilizes ion exchange columns to separate out the various platinum group metals outlined in Appendix A. The ore is first dissolved and then separated through ion exchange methods to obtain the iridium and other PGM's [21-22].

Isotopic Ratios 2.6

Once an element of interest has been chosen and purified, often times the next steps in the production process are isotopic enrichment and irradiation that will produce an activated source. Both of these steps involve both small and large changes in the

isotopic composition of the material. Identifying isotopic signatures in nuclear and radiological material can therefore provide valuable information on the enrichment process used on the sample as well as the method of activation that was used for the isotope which was produced. Small isotopic shifts may even be able to provide very specific information on the neutron spectrum of the reactor that the isotope was activated in and the fluence the sample was exposed to. This information may include the flux of the reactor, the spectrum of thermal and epithermal neutrons, the irradiation time, and decay time. Isotopic analysis can also provide information for determining the age of a sample as well. There have also been examples where, the isotopic composition of the reagents used in the separations process, have been used to identify where the material came from as well [23].

Isotopic Enrichment

Most elements have more than one isotope in their naturally occurring state on earth. When producing a specific isotope there may be another naturally occurring isotope of the same element which would also activate to measureable or high levels. This may not be desired for a number of reasons. The first reason is that the unwanted activation product has a much longer half-life making long term storage and disposal problematic. Another reason to avoid other activation products is that the other products may emit ionizing radiations that would interfere with the intended use of the source or be harmful to the source user. For instance, a source that is produced for use where an alpha emission is desired but the other isotope product produces gamma or beta emissions could be harmful or interfere with the intended use of the source. The unwanted activated product may also emit the desired form of ionizing radiation but at

too high of energy. This is a particular concern when making medical isotope where low energy emissions are desired so that the emitted radiation deposits in the desired area and does not damage healthy tissue in other parts of the body.

There are multiple methods used for isotopic enrichment. Early methods of enrichment included the use of Calutrons and gaseous diffusion. These methods are most commonly known for the enrichment of U-235 during World War II and the making of the first atomic bombs [24]. More recently centrifugation has become the method used for the enrichment of most materials [25]. It is much more space efficient and cost effective. Modern electromagnetic separators are also beginning to be used more frequently. These are smaller more efficient methods which use similar techniques as Calutrons. There are both government and private organizations which enrich materials which can then be purchased for use by both private and government organizations [25].

Iridium-192 enrichment has traditionally been done through gaseous centrifugation. Natural iridium contains 37% ^{191}Ir and 63% ^{193}Ir. Iridium is most commonly enriched to just above 80% ^{191}Ir enrichment from the 37% natural abundance for medical sources. This iridium is currently only produced by a private company in the Netherlands though it has been produced by Oak Ridge National Laboratory in the past [25].

Reactor Neutron Spectrum

The amount and mode of neutron activation of a material is affected by several variables in a reactor. Changes in the flux, fluence and energy spectrum can lead to changes in rate of production of different isotopes in a sample. These variables can

therefore leave behind characteristic signatures that can be measured for fingerprinting of a material.

Information about the flux, fluence and neutron energies in the case of neutron capture can be derived from isotopic information utilizing the first order differentials given in equation 2.1 [26];

$$\frac{dN_i}{dt} = \Lambda^*_{i-1} N_{i-1} - \Lambda_i N_i$$

where,

$$\Lambda^*_{i-1} = (\sigma_{th}\Phi_{th} + \sigma_{epi}\Phi_{epi})$$

And,

$$\Lambda_i = \left(\sigma_{th}\Phi_{th} + \sigma_{epi}\Phi_{epi}\right) + \lambda_i$$

Equation 2.1: The amount of activity produced when an isotope is paced into a neutron field accounting for cross-section (σ), flux (Φ), number of atoms (N), and decay constant (λ).

The neutron flux is the number of neutrons that pass through a given area per second. The cross section is a measurement of the probability that the nucleus of an atom in the sample matrix will absorb a neutron and is reported in the unit of barns (b) where 1b = 1 x 10^{-24} cm^{-2}. The neutron spectrum in a reactor can change over time due to many variables. Accounting for these changes by integrating the flux of a reactor over a given period of time is known as the fluence. Every reactor also has an energy spectrum where there are varying number of neutrons at given energies as seen in figure 2.5 [27].

Each isotope has specific cross sections for both the thermal and epithermal neutron capture reactions. A change leading to an increase or decrease in either the thermal or epithermal neutrons present in a reactor will therefore be seen in the amount and ratios of isotopes produced and depleted in an irradiated sample. Quantification of

the isotopes and isotopic ratios in a sample can therefore be used to identify characteristics of the neutron spectrum used for the activation of a material.

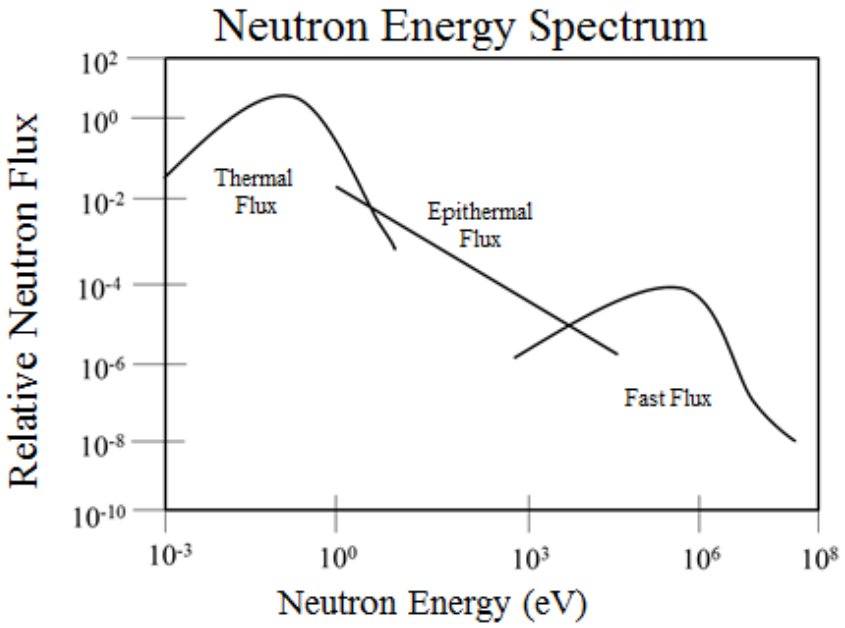

Figure: 2.5 A typical reactor neutron energy spectrum showing the various components used to describe the neutron energy regions.

This figure demonstrates what a typical energy spectrum for reactor produced neutrons looks like. As can be seen the lower energy thermal and epithermal neutrons are far more prevalent. These neutrons are the neutrons most responsible for activation of a sample matrix within the neutron field in a reactor.

Chronometry/Age Dating 2.7

Determining the age of a sample, can also be an important measurement for the attribution of a source. There are multiple characteristic time periods that can be referred to with respect to age when speaking about the age of a source [1-3, 28]. The ages that can be measured include the irradiation time as well as the time since irradiation. Measurement of both time periods are important for attribution purposes. Determining

the amount of time since irradiation can give information on the location that the source could have possibly been irradiated as well as those that might have been responsible for the source. The irradiation time may also provide information to where the source may have originated.

Decay Time of Source

The decay time of a sample can be defined as the amount of time that has elapsed since the end of the sources irradiation. This is done by using the exponential decay law to determine the amount of material that has decayed. An example of the way age can be determined is through the decay of ^{192}Ir given in equation 2.2.

$$^{191}_{77}\mathrm{Ir} + ^{1}_{0}\mathrm{n} \longrightarrow ^{192}_{77}\mathrm{Ir} \longrightarrow ^{192}_{78}\mathrm{Pt} + ^{0}_{-1}\beta + \gamma$$

Equation 2.2: The balanced reaction for the neutron absorption and subsequent beta and gamma decay of iridium to stable platinum.

As can be seen, ^{191}Ir absorbs a neutron in the reactor to make activated ^{192}Ir. The unstable Ir-192 decays via beta and gamma emission following the law of exponential decay described in equation 2.3. Iridium-192 has a half-life of 73.83 days therefore, over the course of 73.83 days the amount of ^{192}Ir remaining will continue to be reduced by half. After 10 half-lives, over 99.9% of the original activity will have decayed to a stable isotope.

$$A = A_o e^{-\lambda t} \qquad N = N_o e^{-\lambda t}$$

Equation 2.3: The amount of activity after decay from an initial activity (Ao) to time (t) as governed by the decay constant (λ).

Platinum-192 is a low abundant isotope naturally accounting for only 0.2% of all natural Pt on earth. Quantifying the amount of ^{192}Pt found in a sample can be used to calculate the amount of ^{192}Ir that has already decayed. Quantifying the amount of ^{192}Pt present in a

sample isotope ratios can be measured by quantifying the amount of other Pt isotopes present in the sample such as ^{195}Pt (33.832%), ^{196}Pt (25.242%), and ^{198}Pt (7.163%) as well. With these ratios isotopic shifts can be measured in order to quantify how much of the ^{192}Pt was originally in the sample and how much is now present due to the decay of ^{192}Ir. Once this is quantified equation 2.2 can be used to calculate the amount of time needed to produce the amount of ^{192}Pt that was found. This time is the decay time.

Irradiation time

A method that can be used for the estimation of the irradiation time of the source is to look at the shift in the isotopic ratios of the materials used. Each isotope is likely to have a different cross section therefore they activate at different rates. An isotope with a larger cross section will activate at a higher rate and will be depleted in relation to the isotope with a smaller cross section. By using the formula in equation 2.4, the irradiation time can be estimated.

$$\frac{^{191}N = {}^{191}N_o \exp(-(\Phi_{th}\sigma_{ep} + \Phi_{th}\sigma_{ep})t)}{^{193}N = {}^{193}N_o \exp(-(\Phi_{th}\sigma_{ep} + \Phi_{th}\sigma_{ep})t)}$$

Equation 2.4: Computation of the shift in the isotopic ratio due to the rate of absorption of neutrons during activation.

N and No are representative of the number of atoms at time t and before irradiation, respectively. The terms Φ and σ are the neutron flux and cross sections for the given isotope. If the flux, cross sections, initial, and final amounts of each isotope can be estimated then, the time of irradiation can be calculated. From this information not only

can the irradiation time be estimated, the decay can be calculated using equation 2.2 and the initial activity of the source using equation 2.3 can be estimated as well.

Conclusions 2.8

There are many different chemical and physical characteristics that are present in radiological materials that can be used for the determination of the origin, decay time, irradiation time, and irradiation environment of a source. These identifiers include both elemental and isotopic quantification of the bulk and trace elements/isotopes in the sample matrix. The information provided could in turn then be used to help in attribution of a lost, stolen, or weaponized source either pre or post attack.

Chapter 3

ICP-MS and AC Dissolution Method

Introduction 3.1

Trace elemental and isotopic analysis are important measurements that are useful in tracking dangerous or illicit materials. While there are a variety of techniques that can be used for the analysis of materials contained in an RDD, this chapter describes a method for the electrochemical dissolution, and ICP-MS analysis of iridium samples for elemental and isotopic analysis.

Electrochemical Dissolution 3.2

To measure and quantify trace metal impurities and isotopic ratios by ICP-MS the iridium samples must be brought into solution. Because iridium is resistant to attack by the strongest of acids, including concentrated HCl, HNO_3, and aqua regia, a simple dissolution of the metal in acid is not sufficient. A review of the literature reveals that a suitable method of dissolution of iridium is through electrochemical dissolution [29]. Alternative methods of dissolution involve high temperature sintering [29] which is not as ideal for work in a hot cell environment as electrochemical dissolution because of the limitations of remote handling as well as the use of high temperatures and dangerous gases.

As demonstrated in the work of Styrkas et al., iridium cannot be brought into solution using direct current (DC or half-wave) electrochemical dissolution (table 3.1) [29]. This is due to the fact that with only anodic dissolution the iridium is oxidized to the +4 state and then IrO_2 forms on the surface of the metal passivating the surface and

stopping any further dissolution [30]. The cathodic half period in alternating current (AC or full wave) dissolution is needed to reduce and remove the iridium (IV) oxide surface layer. Anodic dissolution may then resume and more dissolution occurs before the surface is again passivated. This cyclical process allows the anodic dissolution to continue as long as AC current flows through the system/cell.

	Dissolution Rate Full-wave (mg/hr*in^2)	Dissolution Rate Half-wave (mg/hr*in^2)	Current Density Full-wave (amps/cm^2)	Current Density Half-wave (amps/cm^2)
Gold	103	998	0.62	0.46
Cadmium	2550	5172	0.62	--
Copper	2426	2078	0.77	0.38
Indium	3657	2070	0.62	0.62
Iridium	**22**	**0**	**0.46**	**--**
Palladium	744	1596	0.54	0.31
Platinum	66	0	0.69	--
Rhodium	172	0	0.46	0.31
Tungsten	62	25	0.46	--

Table 3.1: (Adapted from Reference [30] in table) Rates of Dissolution for various metals in 9M HCl using 60cps alternating current and current densities. As can been seen iridium has the slowest rate of dissolution and cannot be dissolved using half-wave or DC current.

Iridium Dissolution

A dissolution method using alternating current electrochemical dissolution was developed to dissolve iridium. The dissolution was performed in an electrochemical cell designed and built for this project. The cell was made of PEEK (poly-ether-ether-ketone) and graphite electrodes (Alfa Aesar 99.9995% purity). PEEK was chosen for its resistance to acids, stability to ionizing radiation exposure, machinability, and shatter resistance. A foot long solid cylinder of PEEK was purchased and then milled at the university of Missouri research reactors machine shop to internal dimensions of 2.54 cm diameter 7 cm long which makes a cell with ~100mL volume (Figure 3.1). Graphite rods

of .615cm diameter by 15 cm long were chosen as the electrodes in order to reduce the potential of metal contamination into the cell during the dissolution process. The dissolution was done in 9 M HCl (trace metal grade, Sigma Aldrich); this concentration was selected based upon the work of Box et al. [31]. A VARIAC (Variable AC) transformer was used to regulate the current and voltage that was introduced to the cell. Ampere and Voltage meters were also included in the system so that the electrical conditions of the cell could be monitored at all times.

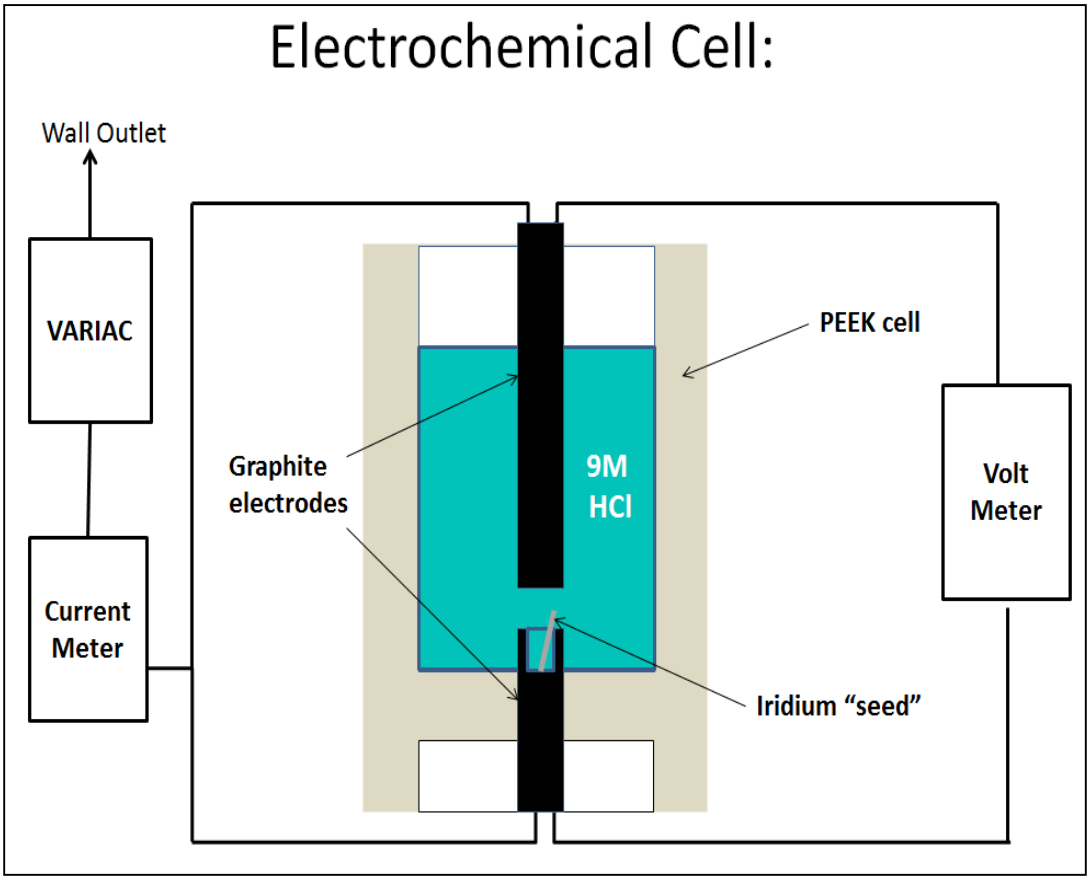

Figure 3.1: Schematic of the electrochemical cell used for the dissolution of iridium. The electrode configuration shown is the configuration found to be most effective for fast dissolution.

There are several factors which regulate the amount of current and voltage that are present in the cell which affects the rate of dissolution. Increases in acid

concentration, voltage and current all lead to an increased rate of dissolution. The distance between the electrodes and position of the gap in the cell also affected the current and voltage. In this work, the AC current density was set between 2 to 5 amps*cm^{-2} and the voltage was set to 3 to 5 V depending upon configuration of the electrodes inside the cell. While higher voltage or current density produced greater dissolution rates, the greater input power resulted in rapid heating of the acid solution to the point of boiling off the HCl acid solution. The conditions of 4V and 2-4 amps*cm^{-2} were found to be the proper balance between higher dissolution rates and keeping the cell from heating too rapidly. While others have used condensers or some other kind of a cooling apparatus for electrochemical dissolution at high powers, lower input powers and slower dissolution rates were used in this work in order to keep the dissolution system as simple as possible for use in a remote environment. Multiple dissolutions of the conditions given above yielded dissolution rates of 1 to 2mg per hour.

Acid blanks were prepared in order to account for contaminants that could be introduced into the dissolved samples reducing the accuracy and precision of the results. Contaminants could come from the acid, the electrochemical cell, sample tubes, or the sample dilution process. Hydrochloric acid was prepared at 9M and an aliquot of 15mL of the acid added to the cell. The acid without any iridium was electrolyzed for 1 hour. The acid was then placed into a sample vial and saved for analysis. After producing an acid blank, an iridium sample was introduced into the cell along with fresh acid from the same batch as the blank. The iridium was then electrolyzed in the acid under the same conditions for 1 hour. The sample was also saved in a vial until time for analysis. This process would be repeated sequentially in triplicate on the same iridium sample to get

three replicate acid blanks and three dissolved iridium samples. Dilutions of all the acid blank and iridium samples were then made and all the samples analyzed at the same time.

Sample Preparation 3.3:

Iridium samples which were dissolved in 9M HCl inside the electrochemical cell were left in 9M HCl to ensure that the H_2IrCl_6 remained in solution until the samples were diluted and analyzed. All vials used for sample storage and dilution were polyethylene tubes (15 mL, Stockwell Scientific). The tubes were pre-cleaned by rocking the vials for 4 hours with ~2mL of 2% HNO_3 (trace elemental grade, Sigma Aldrich). Because of the instability of the platinum group metals in dilute acid solutions, samples were diluted and analyzed on the same day. [301] It is necessary to use dilute acids in order to protect the internal components of the instrument form degradation by the concentrated acid. Sample dilutions were performed gravimetrically using 2% HNO_3 (Sigma Aldrich, trace metal grade). Dilutions of the samples were made in order to have sample concentrations that are optimal for the analysis with the instrument. Dilution factors varied depending upon the estimated iridium concentrations of the electrochemical dissolution samples. For trace impurities analysis, the samples were diluted so that the iridium concentration was in the range of 1 to 5 ppm. For analysis of iridium, the sample was diluted so that the iridium concentration was on the order of 10ppb. Typical concentrations of the iridium in the dissolved samples was on the order of 10 to 300 ppm so dilutions of 20x and 2000x were made for the lower concentrated samples and dilutions of 100x, 1000x, and 10,000x were done when iridium concentrations in the original sample reached concentrations greater than 100 ppm. All acid blanks were diluted 100x prior to analysis.

An internal standard of Sc/In/Tl (High Purity Standards) at a final concentration of 10 ppb was added to all diluted samples. These elements were chosen due to their common use for an internal standard; they also were not expected in the iridium sample causing interference with quantification. Because their masses range from light (Sc at 45 amu) to middle (In at 115 amu) to heavier elements (Tl at 205 amu), this set of internal standards could be used to effectively account for mass bias across a wide range. Once it was determined which impurities where found in the platinum metals group, the internal standard was changed to Cd/Tl (High Purity Standards). This was done because Cd has a first ionization energy closer to the platinum groups than In (table 3.2). Scandium was also no longer used because there were no light elements of interest. This internal standard was added to all samples at 10ppb. Internal standards were used to correct for instrument variation during analysis.

Sc	***Cd***	**In**	**Tl**						
633.1	***867.8***	**558.3**	**589.4**						
Ta	W	Re	Os	Ir	Pt	Ru	Rh	Pd	Au
728.4	758.8	755.8	814.2	865.2	864.4	710.2	719.7	804.4	890.1

Table 3.2: 1st ionization energies of the elements in the internal standards and quantified trace impurities in the iridium sample matrices.

Quantification of the analytes was done with the use of external standards. Dilutions of the standards were made from stock solutions of multi-element solutions (High Purity Standards) found in Appendix B. Each multi-element standard was diluted to concentrations of 1pbb, 5ppb, 10ppb, and in some cases 50ppb dependent upon the expected concentrations of the analytes of interest. In the case of the iridium single element standard dilutions were made at 1ppb, 5ppb, 10ppb, 50ppb, 100ppb, and 1ppm. All external standards also contained the Sc/In/Tl or Cd/Tl internal standards at 10 ppb. A

linear regression of the standards at different concentrations was created and used to quantify the elements in the sample matrix.

Sample Analysis 3.4:

The instrument was tuned and calibrated using a common standard solution and method. The standard solution contained Mg, Sc, In, Pb, and U at 1ppb each in 2% trace metal grade HNO_3. The instrument settings used in the analysis of the dissolved iridium samples are given in table 3.3. A blank wash of 2% HNO_3 as well as a zero point standard containing the internal standard at 10ppb were both used in analysis for a wash and the computation of the limits of detection and quantification.

Quadrupole		High Resolution	
Resolution	300	Resolution	1000
Rf Power	1600W	Rf Power	1400W
Integration time	7 Sweeps - 5 Replicates	Integration time	5 Sweeps – 5 Replicates
Spray Chamber	Quartz Jacketed	Spray Chamber	Quartz Jacketed
Cool Gas	Argon	Cool Gas	Argon
Auxiliary Gas	Argon	Auxiliary Gas	Argon
Sample uptake	1mL/min	Sample uptake	1 mL/min
Flush time	105 sec	Flush time	60 sec
Wash time	60 sec	Wash time	60 sec
Cones	Nickel/Nickel/Nickel	Cones	Nickel/Nickel

Table 3.3: Parameters of the quadrupole and High Resolution ICP-MS instruments used for the analysis of iridium samples.

A list of analytes was created based upon the sample suppliers trace impurity analysis data sheet, from literature information on iridium origins, elements in the same region as iridium on the periodic table, and through selection of elements with similar chemistry to iridium. Table 3.4 lists the elements incorporated into the method of analysis.

Ag	As	Au	B	Bi	Ca	Cr	Cu
Fe	Mg	Mn	Mo	Ni	Os	Pb	Pd
Pt	Rh	Ru	Sb	Sc	Se	Sn	Ta
Te	Ti	W	Zn	Zr			

Table 3.4: List of all elements analyzed for as trace impurities in all iridium samples.

High Resolution Resolving Power

A resolving power of 1,000 was chosen for the first analysis of samples. This resolving power was chosen to have a more selective analysis than a quadrupole without sacrificing signal intensity to the point where trace impurities were not detectable. This resolving power was found to be narrow enough to separate all significant peaks while still having a sensitivity great enough that all trace metal impurities of interest could be quantified. This was verified by looking at each individual spectra and visually verifying that there were no overlapping peaks and that all peaks had sufficient separation and that the data collected was solely due to that specific isotope.

Kinetic Energy Discrimination

Since the trace impurities in the samples were at very low concentrations in the electrochemically dissolved samples, samples with relatively high iridium concentrations needed to be analyzed in order to quantify the trace impurities. In order to not damage the detector with high iridium concentrations, the trace impurities were measured in standard mode with no KED gas in the cell. The same samples were then analyzed in KED mode where the iridium concentration was reduced in the collision cell due to the He atoms reducing the beam signal. Therefore, both the iridium and trace impurities could be measured in the same sample with high precision and accuracy without harming the equipment.

Conclusions 3.5:

An electrochemical cell for the dissolution of iridium metal was developed, built and a method for dissolution created for the dissolving of iridium samples. A method for the analysis of dissolved iridium samples was created for the analysis of iridium and its trace metal and isotopic signatures with ICP-MS instrumentation. The results for this work are given in chapter 4.

Chapter 4

Iridium Results and Discussion

Introduction 4.1

Results from high resolution and quadrupole ICP-MS analysis have been collected for the electrochemically dissolved stable metal iridium, enriched ^{191}Ir, and aged ^{192}Ir samples. Signatures found in the iridium materials are to be used to identify the multiple pieces of information leading to identification of the origin, type of source, activation time, irradiation time, irradiation environment, and time of decay of the source. Dissolutions and analysis with high-resolution and quadrupole ICP-MS measurements have been made with the same iridium wire in triplicate to verify reproducibility of the measured impurities using the developed method. Triplicate samples were also analyzed on both the high resolution sector field and quadrupole ICP-MS instruments to identify any variances between instruments. A standard addition experiment was done in order to confirm the concentration of the elements being measured. Isotope ratios of the iridium and its trace impurities were also measured using quadrupole ICP-MS in order to identify the difference between medical and industry sources as well as the activation conditions.

Stable Iridium Dissolution and Analysis 4.2

Initial conditions used for the dissolution and analysis of the iridium samples described in chapter 3 were used for the analysis of all iridium samples. The dissolution conditions of 1 hour dissolution with 3V and 3amps AC current produced enough iridium that trace elemental and isotopic analysis were possible with the ICP-MS instruments used for this work. These conditions resulted in Ir concentrations of ~100 ppm in a total

solution volume of ~10 mL. The trace elemental concentrations in the dissolution solution were on the order of 1 to 10 ppb which are all above the limit of quantification for the sector field and quadrupole ICP-MS instruments. This relatively short 1 hour dissolution time is critical because it makes fast analysis of a sample in the case of a radiological event possible so that information on the material can be quickly collected and sent to the appropriate authorities.

Alfa Aesar Iridium Analysis

The concentration of Ir and trace elements from three sequential 1 hour dissolutions of the outer layers of the same iridium wire (Sample 1-3), purchased from Alfa Aesar, are given in tables 4.1-4.4. A fourth dissolution of the entire remaining wire (Sample 4) was done after the three initial dissolutions. The total dissolution required 19 hours to dissolve the entire remaining seed. As can be seen Mo, Ru, Rh, W, and Pt were all found at levels above the limit of detection (LOD) for at least 2 of the 3 dissolutions. Each of the elements was quantified with the use of a Sc/In/Tl internal standard (10ppb) and a series of external multi-element standards.

	Sample 1	**Sample 2**	**Sample 3**	**Sample 4**
Ir (mg)	0.85	0.60	0.50	9.70

Table 4.1: Mass of iridium (mg) dissolved in replicate dissolution samples of Alfa Aesar wire.

The data in table 4.1 shows the mass of iridium dissolved in each of the four sample dissolutions. Variations in mass are due to a number of variables which in turn affect the dissolution rate. These variables include; voltage, current, the electrode gap, location of the wire in the cell, “seed” size, amount of acid, and dissolution time.

The concentrations of the trace impurities inside the iridium wire were calculated as micrograms of the PGM (platinum group metal) per gram of iridium. All analytes,

other than Mo, had less than 5% RSD between the measured concentrations in the Ir wire from the three dissolution samples (Table 4.4). In the case of Ru, W, and Pt, multiple isotopes of the trace element were used to determine the concentration of the PGM and helped exclude potential isobaric interferences. Mo and Rh were only measured with the one isotope shown in Table 4.2; Rh has only one stable isotope and the other isotopes of Mo have multiple isobaric interferences.

Isotope	Sample 1	Sample 2	Sample 3
^{95}Mo	2.64E-04	0.00E+00	2.58E-04
^{99}Ru	6.44E-03	3.39E-03	3.14E-03
^{101}Ru	6.76E-03	3.54E-03	3.07E-03
^{103}Rh	1.16E-02	6.07E-03	5.29E-03
^{182}W	1.53E-01	8.31E-02	7.07E-02
^{184}W	1.56E-01	8.44E-02	7.07E-02
^{195}Pt	7.95E+01	4.23E+01	3.76E+01
^{196}Pt	6.89E+01	3.59E+01	3.26E+01
^{198}Pt	5.01E+01	2.54E+01	2.25E+01

Table 4.2: Measured trace metal impurity concentrations (ppm) in the dissolution (solution) Alfa Aesar iridium samples.

Tables 4.2 provides the acid blank subtracted concentration of the trace PGM's in the dilution sample matrix and table 4.3 provides the limit of detection for each analyte, respectively. The limit of detection was determined by three times the standard deviation of the zero point standard. Table 4.4 converts the concentrations of the trace impurities in table 4.2 and the iridium masses in table 4.1 into the concentration of the trace elements in the original iridium wire.

Isotope	Sample 1	Sample 2	Sample 3
^{95}Mo	1.83E-04	2.26E-04	2.29E-04
^{99}Ru	2.00E-04	2.47E-04	2.51E-04
^{101}Ru	1.69E-04	2.09E-04	2.12E-04
^{103}Rh	1.08E-05	1.33E-05	1.35E-05
^{182}W	1.40E-04	1.73E-04	1.75E-04
^{184}W	1.17E-04	1.45E-04	1.47E-04
^{195}Pt	9.84E-02	1.22E-01	1.23E-01
^{196}Pt	1.80E-01	2.23E-01	2.27E-01
^{198}Pt	6.30E-01	7.79E-01	7.91E-01

Table 4.3: Limit of detection (ppm) for trace elements in dilutions of Alfa Aesar iridium samples.

Isotope	Sample 1	Sample 2	Sample 3	Mean	STDEV	%RSD	Alfa Aesar Values
^{95}Mo	<LOQ	<LOD	<LOQ	3	3.6	107	ND
^{99}Ru	69	72	74	72	2.5	3.5	120
^{101}Ru	72	75	72	73	1.7	2.4	120
^{103}Rh	124	129	124	126	2.9	2.3	29
^{182}W	371	399	375	382	15.1	4.0	449
^{184}W	369	397	367	378	16.8	4.4	449
^{195}Pt	241	255	250	249	7.1	2.9	263
^{196}Pt	252	261	261	258	5.2	2.0	263
^{198}Pt	254	257	251	254	3.0	1.2	263

Table 4.4: Measured concentrations (ppm) of trace metal impurities in Alfa Aesar iridium wire.

As can be seen there is good agreement between isotopes of the same elements as well as agreement in element concentrations between all three dissolutions. There is moderate

agreement between the measured concentrations of the trace impurities with the concentration of the trace impurities listed in Alfa Aesar's certificate of analysis.

A secondary concern with the analysis is that both the seed and the dissolution process need to yield consistent results for the concentrations of the trace elements. Dissolving only a fraction of the sample rather than the entire seed or disk is useful in order to have fast analysis which is needed in forensic investigations. Variance in the concentration of analytes in the dissolved samples could be due to the iridium being heterogeneous with the trace impurities having higher concentrations on the outer layers of the sample. Fractionation of the impurities during dissolution from different elements having different dissolution rates could also lead to variances in the concentrations of the impurities. In order to investigate the reproducibility of the dissolution method and what portion of a sample is needed to be dissolved for representative results, data from iridium samples 1-3, listed in tables 4.1, 4.2, 4.3, and 4.4, was used. This data comes from triplicate dissolutions of a portion of the Alfa Aesar iridium wire. The remaining wire sample was then dissolved completely in the electrochemical cell over the course of 19 hours to create sample #4. Analysis of samples 1-4 were all performed on the same HR-ICP-SFMS instrument on the same day as seen in (Table 4.5). There was no significant difference in the elemental composition of the partial dissolution iridium solutions (1-3) and the completely dissolved wire (core). This indicates, that for this iridium source, a partial dissolution provides a representative analysis. The data also suggests that there is not any fractionation in the dissolution process for these particular impurities.

Isotope	Mean Partial	STDEV Partial	%RSD Partial	Full	STDEV Full (LOD)	Alfa Aesar Values
^{95}Mo	3	4	107	3	6	ND
^{99}Ru	72	3	4	72	8	120
^{101}Ru	73	2	2	N/A	N/A	120
^{103}Rh	126	3	2	131	9	29
^{182}W	382	15	4	373	8	449
^{184}W	378	17	4	371	9	449
^{195}Pt	249	7	3	260	4	263
^{196}Pt	258	5	2	261	5	263
^{198}Pt	254	3	1	254	28	263

Table 4.5: Comparison of three sequential partial dissolutions and subsequent complete dissolution of the Alfa Aesar wire. (^{101}Ru isotope was not analyzed (N/A) for measurement of core dissolution due to error in experimental method.)

As already seen, high resolution ICP-SFMS analysis of the iridium provided reproducible data for several impurities including Mo, Ru, Rh, W, and Pt from a sample iridium wire (table 4.1). The presence of these trace impurities was expected due to the similar chemical properties of the platinum group elements. Because their chemical properties are similar to iridium, it would follow that they are the most difficult to separate from iridium and therefore most likely to be some of the more prevalent impurities.

ICP-MS measurements with a NEXION quadrupole instrument (ICP-QMS) were also done to compare the ICP-QMS instrument measurement capabilities to a high resolution instrument. Samples of the Alfa Aesar iridium wire were dissolved in triplicate using the electrochemical cell and method as before. The added advantages of the quadrupole instrument relative to the SF-ICP-MS is the reduced analysis time and the use of an automatic sample loader. Quadrupole instruments in general have lower

sensitivities, faster analysis time, and are also more commonly used [32]. This means that a methodology for the analysis of samples with a quadrupole would be more useful for a greater number of laboratories.

The results of the quadrupole analysis of three dissolutions of the Alfa Aesar wire are given in Table 4.6. The same elements that were observed with the high resolution instrument were detected and quantified with the quadrupole instrument with better precision in most cases.

Isotope	**^{99}Ru**	**^{101}Ru**	**^{103}Rh**	**^{182}W**	**^{184}W**	**^{195}Pt**	**^{196}Pt**	**^{198}Pt**
Mean	62	62	98	349	359	206	204	214
RSD	4.3	7.9	5.5	0.7	0.5	1.5	1.0	3.9

Table 4.6: Triplicate analysis of an individual Alfa Aesar iridium wire with the quadrupole ICP-MS.

AOS Iridium Sample Analysis

A common iridium supplier in America is Alpha Omega Samples (AOS). They produce natural and enriched iridium with an 80% enrichment of ^{191}Ir. Dissolution and analysis methods previously described were used for the natural AOS material. As seen in table 4.7, concentrations of the Pt and the Ru were similar in the samples from different suppliers whereas the concentrations of W, Mo, and Rh were significantly different. These differences could serve as a potential signature to distinguish between suppliers. It can also be noted that there is agreement on the concentrations of the trace impurities using different isotopes.

Isotope	**^{95}Mo**	**^{99}Ru**	**^{101}Ru**	**^{103}Rh**	**^{182}W**	**^{184}W**	**^{195}Pt**	**^{196}Pt**	**^{198}Pt**
Mean	12.5	74	74	65	7.1	8.9	220	223	232
STDEV	0.03	1.2	3.2	13	1.1	0.04	6.7	9.1	5.8
%RSD	0.26	1.7	4.3	20	16	0.49	3.0	4.1	2.5

Table 4.7: The concentration of trace impurities measured with ICP-QMS in triplicate sequential dissolutions of an AOS sample.

ESPI Iridium Analysis

Iridium samples were also obtained from ESPI Materials at two different purities; 3N5 (low purity) and 4N (higher purity). The resulting data (Table 4.8) shows that all of the trace impurities except Mo found in the Alfa Aesar and AOS samples were also present in the ESPI samples. As expected, the trace impurities of Ru and Rh were found to be at lower concentrations in the 3N5 samples. Surprisingly, the concentrations of W and Pt in the 4N samples were found to be higher than the 3N5 sample.

Isotopes	3N5 Mean	3N5 STDEV	4N Mean	4N STDEV
^{99}Ru	16.4	0.5	6.4	0.6
^{101}Ru	15.7	1.2	6.0	0.2
^{103}Rh	111.7	3.3	6.0	0.2
^{182}W	24.0	2.9	170.6	141.1
^{184}W	25.2	2.6	173.6	142.0
^{195}Pt	4.6	2.4	55.5	5.0
^{196}Pt	5.0	0.7	56.1	4.8
^{198}Pt	6.8	6.1	59.4	8.4

Table 4.8: Trace impurities found via ICP-QMS in triplicate sequential dissolutions of grade 3N5 and grade 4N iridium purchased from ESPI materials.

QSA Iridium Analysis

Iridium samples were also obtained from QSA. Samples of both naturally abundant iridium as well as enriched iridium were analyzed. Both samples were dissolved electrochemically following the previously established method. The data for the natural iridium is given in table 4.9.

Isotope	^{99}Ru	^{101}Ru	^{103}Rh	^{182}W	^{184}W	^{198}Pt
Mean	17.9	19.2	29.0	6.8	6.4	52.7
STDEV	2.7	2.4	2.9	2.4	3.0	4.6

Table 4.9: Trace impurities found via ICP-QMS in triplicate sequential dissolutions in QSA natural iridium.

As can be seen all four of the same trace impurities were quantifiable but at lower levels than the iridium from other manufacturers.

Trace Impurities in Enriched Iridium

Samples of enriched ^{191}Ir were obtained from ESPI and QSA and were electrochemically dissolved in triplicate as previously described. The trace impurity results analyzed by ICP-QMS for the two samples are given in tables 4.10 & 4.11. The concentrations given are the mean of all isotopic concentrations measured when more than one isotope was quantified.

	Ru	**Rh**	**W**	**Pt**
Mean	1.4	27	45	35
STDEV	1.1	0.6	6.2	8.1

Table 4.10: Trace impurities found in enriched ^{191}Ir sample from ESPI.

	Ru	**Rh**	**W**	**Pt**
Mean	0.5	0.9	8.3	10.7
STDEV	0.5	0.1	1.9	3.4

Table 4.11: Trace impurities found in enriched ^{191}Ir sample from QSA.

As can be seen, the trace impurities were found to be much lower in the enriched samples than the non-enriched samples. Since the enrichment process selectively removes elements by mass, one would expect to see a decrease in the amount of trace impurities, especially those which have significantly different masses from ^{191}Ir. Concentrations of trace impurities in the enriched samples approached the limit of detection which is reflected in the large standard deviation in the results.

An isotopic analysis of the samples was also performed. As can be seen in figure 4.1 and table 4.12, the enriched samples have an enrichment of ^{191}Ir to just above 80% which is consistent with manufacturer information.

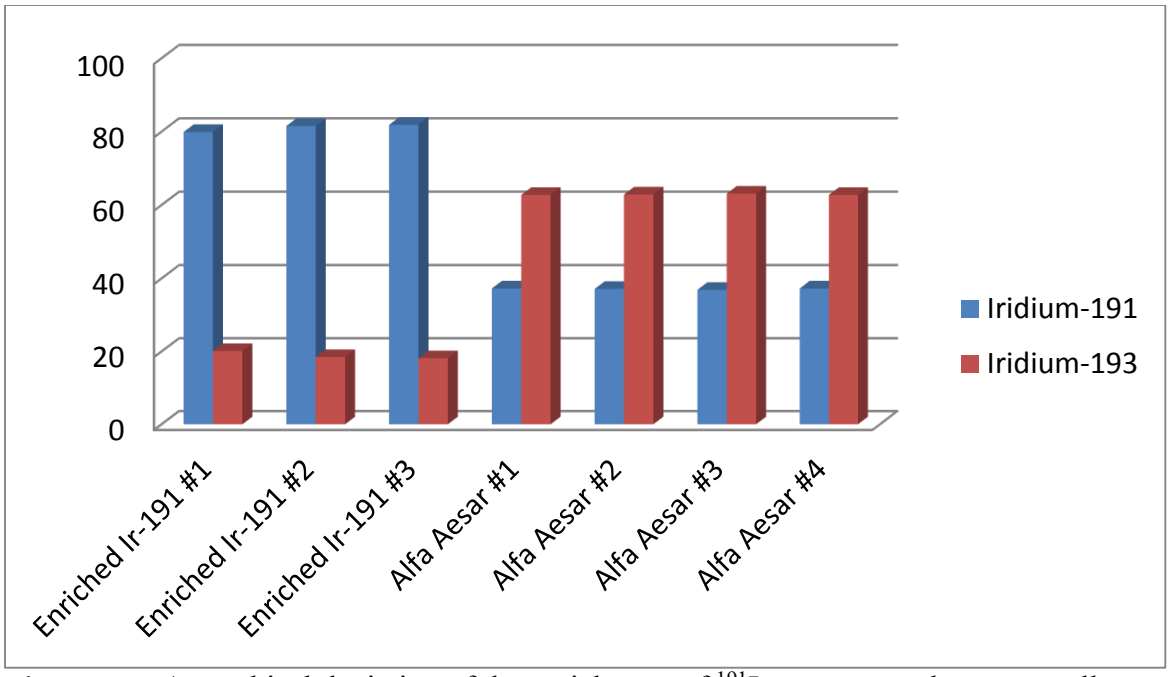

Figure 4.1: A graphical depiction of the enrichment of ^{191}Ir as compared to a naturally abundant iridium single element standard.

	^{191}Ir #1	^{191}Ir #2	^{191}Ir #3	^{Nat}Ir #1	^{Nat}Ir #2	^{Nat}Ir #3	^{Nat}Ir #4
Ir-191	79.9	81.5	81.9	37.3	37.1	36.9	37.3
Ir-193	20.1	18.5	18.1	62.7	62.9	63.1	62.7

Table 4.12: Isotopic abundance for the ESPI enriched ^{191}Ir sample and naturally abundant Ir from a single element standard.

Medical ^{192}Ir sources typically come in the form of a "seed" with a mass of about 5 mg while industrial sources are disks with a mass of about 20 mg. These differences are great enough that the shape and mass of the material should be sufficient information to identify the type of source used without any dissolution or ICP-MS analysis needed. However, as a means of verification or in the event the material has been ground to a powder, the isotopic measurements from above could be used to identify the type of source that has been obtained. The enrichment of ^{191}Ir varies depending on whether the iridium source is for medical or industrial use therefore, isotope ratio measurements are important for identification of the type of radioactive source that has been found.

Activated Iridium Samples 4.3

Following the analysis of the natural and enriched iridium samples, the established methods were then applied to analysis of decayed ^{192}Ir sources. Samples included radiography disks from multiple sources as well as a medical seed. All sources were multiple years old with total activities in the low micro curie range.

Analysis of Activated Disks

Multiple spent disks from ^{192}Ir sources produced by QSA were obtained from Idaho National Laboratory's sealed source recovery program. A single disk from one source produced in 2008 was obtained as well as 12 disks from a single source produced in 2009. As expected from the analysis of the cold iridium samples, there are multiple platinum group metals including Ru, Rh, W, and Pt at concentrations in the 10's to 100's of ppm in the disks (tables 4.13 and 4.14). These values vary between the two sources which quite possibly contain iridium from different suppliers and may have even been irradiated in different reactors.

Element	Ta	Ru	Rh	W	Pt
[PMG]	6170 ± 560	249 ± 4.5	24 ± 19	182 ± 10	220 ± 7

Table 4.13: Concentration of platinum group metals found in triplicate dissolutions in QSA source #38946239

Element	Ta	Ru	Rh	W	Pt
[PMG]	162 ± 26	119 ± 15	18 ± 9	127 ± 7	n/a

Table 4.14: Concentrations of platinum group metals found in triplicate dissolutions in disk 1 of QSA source #8423798437 (Pt was not analyzed for this sample)

Analysis of Activated Seed

A spent iridium seed weighing approximately 5 mg which was enriched in ^{191}Ir and irradiated at the University of Missouri's Research Reactor was obtained for analysis

and compared to the activated disks from QSA. Dissolution of the seed was difficult due to the small size of the sample. Triplicate dissolutions were done and results of the analysis are given in table 4.15. The trace impurities in the medical seed are, for the most part, at concentrations lower than the disks.

Label	Mean	STDEV	%RSD
^{99}Ru	10.9	5.3	48.9
^{101}Ru	26.7	15.0	56.4
^{103}Rh	12.9	1.9	14.4
^{181}Ta	8.4	2.5	29.5
^{182}W	110	105	95
^{184}W	106	102	96
^{186}W	107	99	93
^{198}Pt	137	42	31
^{197}Au	0.7	1.2	173

Table 4.15: Analysis of triplicate dissolutions of the medical ^{192}Ir seed on back-to-back days.

The enriched samples had lower concentrations of the trace impurities than the natural samples, especially the elements far from iridium in mass (i.e. Mo, Ru, and Rh). The trace impurities of the seed in table 4.15 are higher than the trace impurities found in QSA and ESPI enriched seeds but are lower than the trace impurities in the natural (non-irradiated) iridium and disk sources which is consistent with the enrichment process removing some of the impurities. The observed trend where the light elements are removed at a greater rate than the elements close to mass in iridium does appear to be present in the medical seed as well. Another interesting note is that there was no increase in ^{182}W that was present in the radiography disks. This can be explained by the ^{181}Ta concentration being much lower in the medical seed than the industrial disks making the production of ^{182}W through neutron capture on ^{181}Ta less likely.

Accuracy, Precision and Robustness 4.4

In order to provide information on a nuclear event that is to be used in a forensic investigation, it is important to know what level of confidence can be given to the data that is provided to the investigating authorities. With a robust statistical analysis of the data, the sensitivity of the measurements can be determined and in turn the confidence in which two samples can be differentiated established.

Standard Addition

A standard addition experiment was performed to identify potential biases in quantification of the analytes measured in the dissolution and analysis process. A multi-element standard containing Rh and Pt was added to the HCl solution before electrochemical dissolution was performed on a piece of the previously analyzed Alfa Aesar wire. Aliquots containing enough analyte to make solutions of 0 ppb, 20 ppb, 40 ppb, and 80 ppb of additional PGM were added. One hour dissolutions of the iridium and iridium + PGM spike solutions were performed and analysis done as previously described. Results for the platinum group standard addition are given below. As can be seen in figure 4.2 there is agreement for all three measured Pt isotopes. The results for Rh and Pt by standard addition agree, within error, with the results using external standards (Table 4.16).

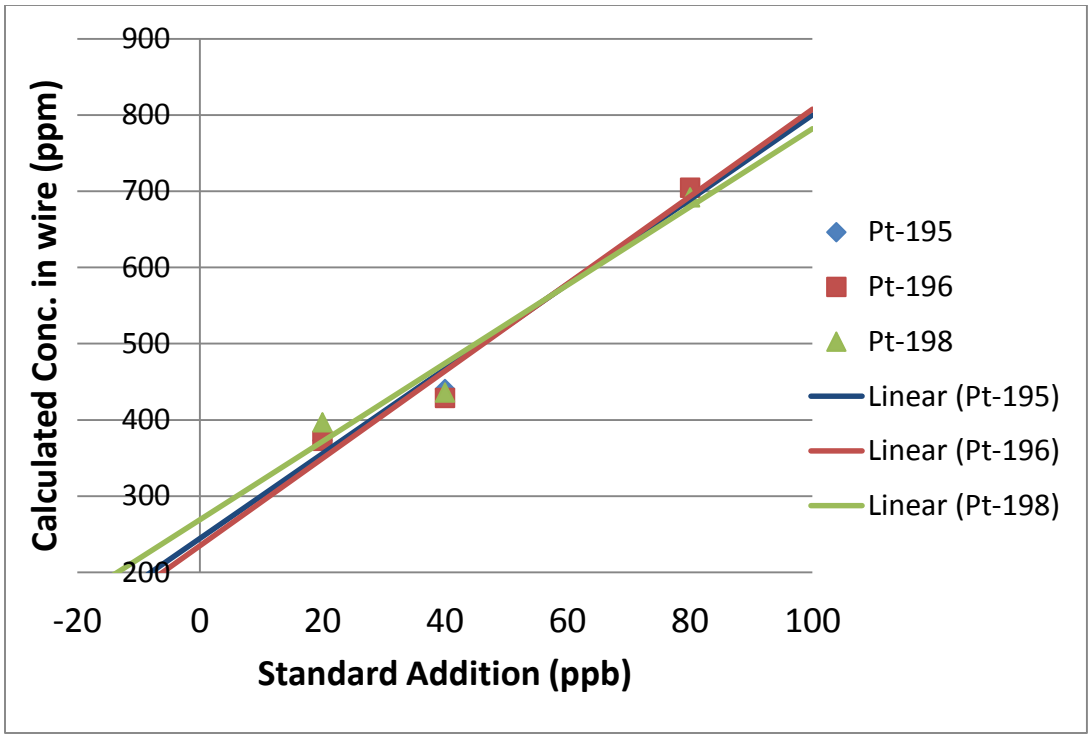

Figure 4.2: Standard Addition plot for three platinum isotopes used for the analysis of trace impurities in Alfa Aesar wire.

	Rh	**Pt**
External Standards	127 ± 6.4	254 ± 16.5
Standard Addition	136 ± 6.8	250 ± 17.5
% Difference	7.1	1.6

Table 4.16: Concentration of Rh and Pt in Alfa Aesar wire measured with external standards and by standard addition.

Precision and Robustness

In order to verify the precision and robustness of the method, new electrochemical dissolutions were performed on the ^{192}Ir disk source from QSA. Consecutive 1 hour dissolutions were performed on the disk in triplicate on two consecutive days. The two day experiment (six dissolutions) was then repeated 6 months later on the same QSA disk sample. All dissolutions were done sequentially on the same disk. Performing three replicate dissolutions on the same day provides information on the precision of the

measurement due to variability in the dissolution and analysis process from one sample dissolution to another. Performing triplicate dissolutions on two different days and then months later provides information on the robustness of the technique due to variability of results from day to day as well as long term variances in the method.

Dilutions of the dissolved samples were made with 3% HNO_3 and then analysis was performed same day with ICP-QMS. The ICP-QMS instrumental parameters and data analysis were performed in the same manner as described above.

3/31/2014				4/1/2014			April		
Isotope	Mean	STDEV	%RSD	Mean	STDEV	%RSD	Mean	STDEV	%RSD
^{95}Mo	26.0	0.4	1.5	24.8	0.9	3.6	25.4	0.8	3.3
^{99}Ru	207	12	6	206	20	10	206.5	0.7	0.3
^{101}Ru	213	9	4	215	20	9	214.0	1.4	0.7
^{103}Rh	11.5	0.7	5.7	11.7	1.6	13.8	11.6	0.1	1.2
^{182}W	189	17	9	182	20	11	185.5	4.9	2.7
^{184}W	92	3	4	77	20	26	84.5	10.6	12.6
^{198}Pt	180	15	8	182	29	16	181.0	1.4	0.8

10/23/2014				10/24/2014			October		
Isotope	Mean	STDEV	%RSD	Mean	STDEV	%RSD	Mean	STDEV	%RSD
^{95}Mo	ND	ND	ND	ND	ND	ND	ND	ND	ND
^{99}Ru	221	5	2	200	10	5	210.5	14.8	7.1
^{101}Ru	216	8	4	193	7	4	204.5	16.3	8.0
^{103}Rh	10	0	4	9.1	0.8	8.6	9.6	0.6	6.7
^{182}W	223	9	4	204	13	6	213.5	13.4	6.3
^{184}W	112	9	8	102	2	2	107.0	7.1	6.6
^{198}Pt	240	1	1	207	20	9.5	223.5	23.3	10.4

Table 4.17: Data collected for the analysis of triplicate samples on back to back days performed months apart.

Table 4.17 presents the quantified amounts of each impurity for the precision and robustness tests. The mean (n=3), standard deviation, and relative standard deviations of

each days results are given. As can be seen in table 4.17 the same isotopic shift appears for tungsten in this irradiated sample while all other impurities do not show measurable differences in isotopic abundance. There appears to be agreement from day to day analysis of each of the materials as well as long term differences. The boxes in gray in table 4.17 show the variance in the measurement of the trace impurities of the iridium samples as measured on two days back-to-back. The quantification of the variance is the precision with which the measurement being made has. Precision for the measurements for the quantification performed in April was better than the quantification in October. The concentrations of many of the trace impurities on 10/23/2014 were all a slightly higher than the other measurements suggesting that there may have been an under-quantification in the amount of iridium in those samples contributing to the lower precision of October's results.

The data from the 4 experiments can also be combined to identify the variance over a greater period of time (table 4.18). This quantification is the robustness of the measurements.

	April			October			Final		
Isotope	Mean	STDEV	%RSD	Mean	STDEV	%RSD	Mean	STDEV	%RSD
^{95}Mo	25.4	0.8	3.3	ND	ND	ND	25.4	ND	ND
^{99}Ru	206.5	0.7	0.3	210.5	14.8	7.1	208.5	2.8	1.4
^{101}Ru	214.0	1.4	0.7	204.5	16.3	8.0	209.3	6.7	3.2
^{103}Rh	11.6	0.1	1.2	9.6	0.6	6.7	10.6	1.4	13.7
^{182}W	185.5	4.9	2.7	213.5	13.4	6.3	199.5	19.8	9.9
^{184}W	84.5	10.6	12.6	107.0	7.1	6.6	95.8	15.9	16.6
^{198}Pt	181.0	1.4	0.8	223.5	23.3	10.4	202.3	30.1	14.9

Table 4.18: The robustness of the experimental data from April and September.

The robustness of the measurements is most accurate for the Ru at 3.2%RSD while one isotope of W has the most variance with 16.6% RSD over the four measurements.

Sample Stability

As stated in chapter 2, iridium is one of the most difficult metals to dissolve and keep in solution. A concern is that if samples are diluted in nitric acid and left in solution for more than a few hours the iridium will fall out of solution. The stability of the prepared samples was investigated by dissolving 6 iridium samples and leaving them in concentrated (9M) HCl until the morning of analysis. On the morning of analysis (Day 1) the dilutions were made in 3%HNO_3 and analysis performed as soon as all samples were prepared. Samples were analyzed with the ICP-QMS and the iridium concentrations quantified. The samples were left untouched and analyzed again the following two days (Day 2 and Day 3).

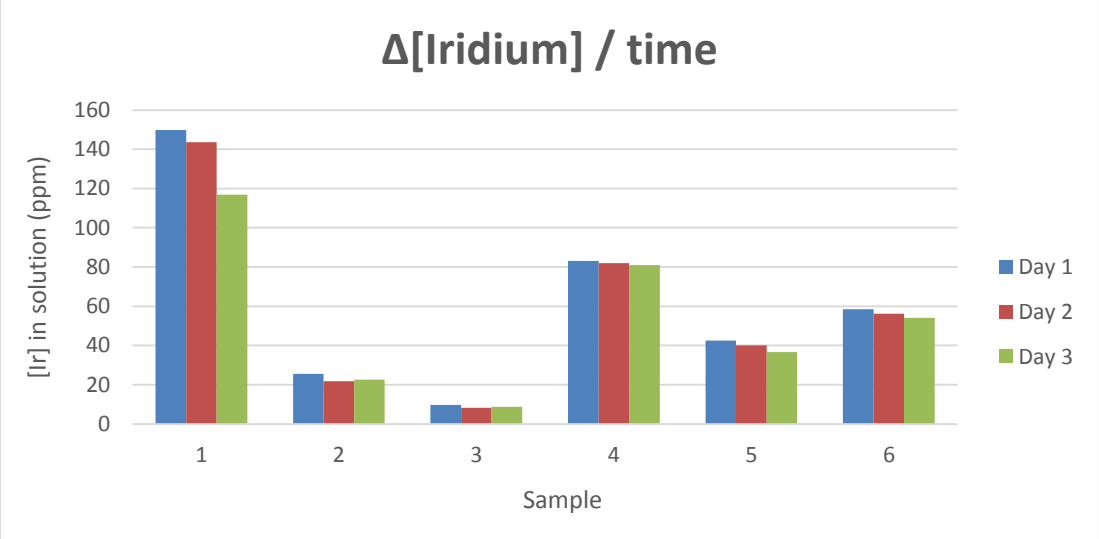

Figure 4.3: The quantified amount of iridium from 6 different dissolved iridium samples and measured at three times post dilution.

The data in figure 4.3 shows that there is some loss of iridium in solution over the course of three days when left in dilute acid. This is most visible for samples 1, 5, and 6. It is therefore important to perform analysis within 12 to 24 hours of dilution.

Irradiation Conditions 4.5

Along with the elemental impurities in the activated sample, the isotopic composition of the samples has a variety of characteristics as well [8, 9]. The ICP-QMS data indicates that there are multiple elements with large isotopic shifts in their isotope ratios in the activated samples. This is expected anytime a material is irradiated to high fluences in a high neutron flux environment.

Both the iridium and the trace impurities will activate and cause isotopic shifts from the natural material. As shown in table 4.19, an isotopic shift in the iridium isotope ratios was observed in the QSA disk sources. The naturally abundant iridium was measured using a single element iridium standard and compared to the isotopic abundances in the activated sample. The lowering of the $^{191}Ir/^{193}Ir$ ratio is expected because ^{191}Ir has a larger neutron cross section and will "burn-up" at a faster rate than ^{193}Ir (figure 4.4).

	^{191}Ir Single Element Standard	**^{193}Ir Single Element Standard**	**^{191}Ir Activated Sample**	**^{193}Ir Activated Sample**
Mean	37.1	62.9	27.0	73.0
STDEV	0.17	0.17	0.53	0.53
%RSD	0.45	0.26	1.97	0.73

Table 4.19: Iridium isotope abundances in the Ir standard and the activated Ir QSA sample. Results are the average of triplicate dissolutions on consecutive days.

This isotopic shift can be used to identify the irradiation time and initial activity of the source. The irradiation time can be determined through equation 4.1.

$$\frac{N_t^{191} = N_o^{191} e^{-(\sigma_{th}\Phi_{th} + \sigma_{epi}\Phi_{epi})t}}{N_t^{193} = N_o^{193} e^{-(\sigma_{th}\Phi_{th} + \sigma_{epi}\Phi_{epi})t}}$$

Equation 4.1: The first order differentials for the rate of burn-up of ^{191}Ir and ^{193}Ir.

Using the natural abundance of iridium for the number of ^{191}Ir atoms (N_o^{191})and number of ^{193}Ir atoms (N_o^{193}), the measured isotopic shift for the number of ^{191}Ir atoms at time t (N_t^{191}) and the number of ^{193}Ir atoms at time t (N_t^{193}), and an estimated thermal and epithermal fluxe of $\Phi_{th} = 1x10^{14}$ and $\Phi_{epi} = 1x10^{13}$ the irradiation time t can be calculated. Using the ICP-QMS data in table 4.14 the irradiation time is calculated to be 35 days. This is consistent with a typical QSA radiography source which is irradiated for 30-40 days [2].

Taking the estimated irradiation time and conditions, the initial activity of the source can also be estimated through the standard sample activation calculations. The activity of the source under the assumed fluxes and irradiation time of 35 days would produce a source with approximately 110 Ci of activity. According to QSA records which have been disclosed for this report, the disk had an activity of 100 Ci a few weeks after irradiation. With a 73.83 day half-life, the 110 Ci initial activity and 100 Ci measurement weeks later are in agreement.

Other isotopic shifts caused by the specific irradiation conditions is the shift in the isotopic ratios of the minor constituents of the material. A shift in the ratios ε^{195}Pt/^{198}Pt, ε^{196}Pt/^{198}Pt, and ε^{195}Pt/^{198}Pt was observed; the measured Pt isotope ratios in the irradiated QSA disk are reported in table 4.20. There is an increase in the amount of ^{195}Pt and ^{196}Pt (table 4201) which can be produced through a variety of routes as shown in figure 4.4.

The rate at which each is produced can be a sensitive signature to the environment in which the material was irradiated.

Sample	$^{195}Pt/^{198}Pt$	$^{196}Pt/^{198}Pt$	$^{195}Pt/^{196}Pt$
ε Natural	4.72	3.52	1.34
ε QSA Disk	38.6 ± 4.3	3.07 ± 0.28	12.6 ± 0.3

Table 4.20: Shift in platinum isotope ratios for triplicate dissolutions as measured with ICP-QMS.

The production of the ^{195}Pt and ^{196}Pt isotopes is believed to be from the neutron capture and beta decay pathways illustrated in figure 4.4.

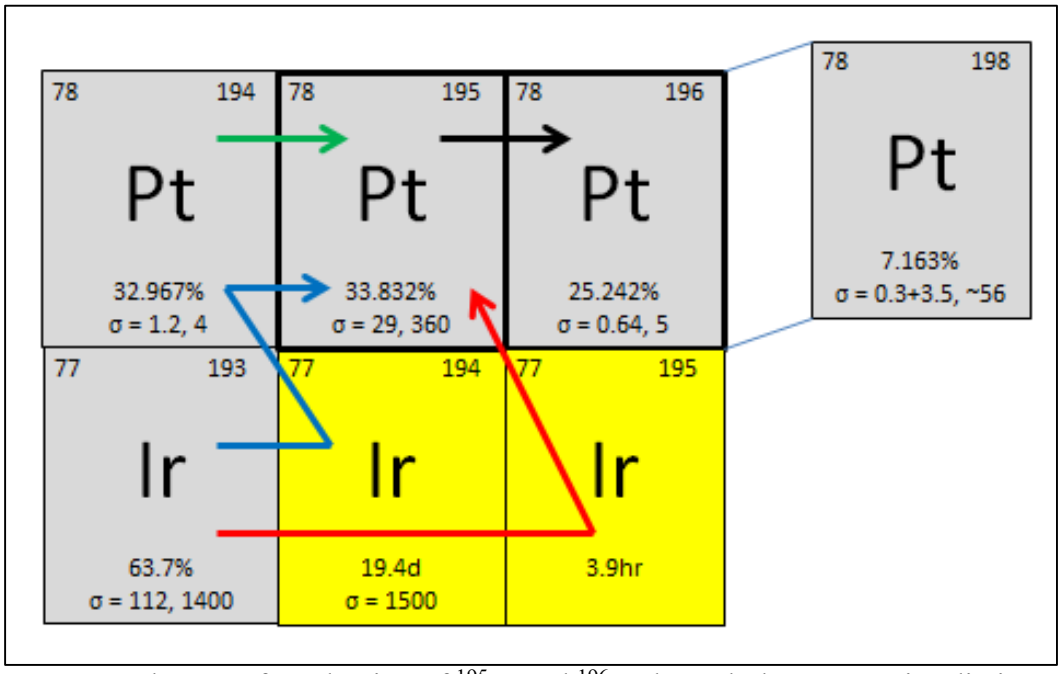

Figure 4.4: Pathways of production of ^{195}Pt and ^{196}Pt through the neutron irradiation of iridium.

The rate of production of ^{195}Pt from each of the colored pathways in Figure 4.7 were calculated with Bateman equation and are given in table 4.N.

Production	Red (double neutron capture)	Blue (n capture, beta, n capture)	Green (n capture natural Pt)	Black (Loss of 195Pt)
dN/dt	4.05×10^{16}	-4.05×10^{14}	2.04×10^{12}	-3.15×10^{15}

Table 4.21: The rate of change in the number of atoms of ^{195}Pt at t = 35 days.

From the data in table 4.21 it is clear that the primary production path of ^{195}Pt, and in turn ^{196}Pt, should be from the double neutron capture of ^{193}Ir to ^{195}Ir which then beta decays to the ^{195}Pt. This is because the ^{194}Ir has a half-life (19.4 days) which is short in relation to the length of the irradiation time (30-40 days) which means it approaches saturation early in the irradiation. ^{194}Ir also has a very large cross section making another neutron capture very likely. The direct production of ^{195}Pt from ^{194}Pt is less likely because of the small cross section for this reaction and because of the small concentration of Pt in the Ir sample. The likely production path of ^{195}Pt can be seen by the blue arrow in figure 4.4 and the nuclear reaction is as follows in equation 4.2;

$$^{193}_{77}\mathrm{Ir} + {}^{1}_{0}\mathrm{n} \xrightarrow{\text{Capture}} \boldsymbol{^{194}_{77}Ir} + {}^{1}_{0}\mathrm{n} \xrightarrow{\text{Capture}} \boldsymbol{^{195}_{77}Ir} \xrightarrow{\beta\ \text{Decay}} {}^{195}_{78}\mathrm{Pt} + {}^{0}_{-1}\beta$$

Equation 4.2: Production of ^{195}Pt through double neutron capture then β decay of ^{193}Ir. (Italicized and bold isotopes are radioactive)

The production of the ^{196}Pt has only one possible production mode which is through the neutron capture of both the natural ^{195}Pt and the newly produced ^{195}Pt from the activation of the iridium given in equation 4.3;

$$^{195}_{78}\mathrm{Ir} + {}^{1}_{0}\mathrm{n} \longrightarrow {}^{196}_{78}\mathrm{Pt} + {}^{1}_{0}\mathrm{n} \longrightarrow \boldsymbol{^{197}_{78}Pt}$$

Equation 4.3: The single route of production and loss of ^{196}Pt in a neutron rich environment. (Italicized and bold isotopes are radioactive)

The isotope shifts from the ICP-QMS experimental data can be compared to the expected amount of each isotope produced under different irradiation conditions. The Bateman equation for first order reactions including double neutron capture is;

$$\frac{dN_i}{dt} = \Lambda^*_{i-1} N_{i-1} - \Lambda_i N_i$$

Equation 4.4: The Bateman equation for the change in the number of atoms in nuclear reactions.

where, $\Lambda_{i-1}*N_{i-1}$ is the rate of production of isotope i and $\Lambda_i N_i$ is the rate of disappearance of the isotope i. The exact solution for the calculation of double neutron capture activation is [35-38];

$$N_n(t) = \Lambda_1 \Lambda^*_2 \ldots \Lambda^*_{n-1} N^0_1 \sum_1^n C_i e^{-\Lambda_i t}$$

where,

$$C_i = \prod_{j=1}^{j=n} (\Lambda_j - \Lambda_i) \ (j \neq i).$$

Equation 4.5: The Bateman equation for the rate of change in production of the number of atoms of a given isotope.

The time in this case is the irradiation time. A specific application for this calculation is the computation of the production of ^{195}Ir from the double neutron capture and beta decay of ^{193}Ir (equation 4.3). In this case the number of ^{195}Pt atoms as a function of time is;

$$N_{195} = \Lambda_{193} \Lambda^*_{194} N^0_{193} \left[\frac{e^{-\Lambda_{193} t}}{(\Lambda_{194} - \Lambda_{193})(\Lambda_{195} - \Lambda_{193})} + \frac{e^{-\Lambda_{194} t}}{(\Lambda_{193} - \Lambda_{194})(\Lambda_{195} - \Lambda_{194})} + \frac{e^{-\Lambda_{195} t}}{(\Lambda_{193} - \Lambda_{195})(\Lambda_{194} - \Lambda_{195})} \right]$$

Equation 4.6: The exact Bateman solution to the double neutron capture and beta decay of ^{193}Ir to ^{195}Pt.

where, Λi is the rate of loss of an isotope and Λ_i^* is the rate of loss of an isotope in the production path being calculated and t is the irradiation time [35]. An example for the case above in the double neutron capture of ^{193}Ir to ^{195}Ir before the beta decay to ^{195}Pt where, Λ_{194} and Λ_{194}^* can be defined as;

$$\Lambda_{194} = \lambda^{\text{Ir-194}}\text{N} + {}^{\text{Ir-194}}\text{N}[\sigma_{\text{Th}}\Phi_{\text{Th}} + \sigma_{\text{R}}\Phi_{\text{R}}]$$

and,

$$\Lambda_{194}^* = {}^{\text{Ir-194}}\text{N}[\sigma_{\text{Th}}\Phi_{\text{Th}} + \sigma_{\text{R}}\Phi_{\text{R}}]$$

Equation 4.7: The rate of loss of the number of ^{194}Ir atoms and the number of ^{194}Ir atoms lost in the production of ^{195}Ir.

As can be seen, Λ_{194} represents the loss of ^{194}Ir atoms through every possible mode of depletion. The term Λ_{194}^* represents only the loss of the ^{194}Ir atoms due to neutron capture which is the production pathway of depletion being calculated in the reaction (equation 4.4) [35]. To account for all possible production of ^{195}Pt, all different potential modes of production and loss of ^{195}Pt must be calculated and then summed.

Along with increases in the amount of Pt isotopes, there is also an increase in the amount of ^{182}W in relation to ^{184}W and ^{186}W as can be seen in table 4.22. There is an increase where the amount of ^{182}W roughly doubles. This cannot be due solely through neutron capture of W based upon the thermal and resonant cross sections for the various tungsten isotopes.

Sample	**^{182}W/^{184}W #38946239**	**^{182}W/^{184}W #8423798437**
ε Natural	0.9	0.9
ε ^{192}Ir Disk	1.7 ± 0.1	0.84

Table 4.22: Isotopic shift in ^{182}W/^{184}W abundance in activated QSA radiography disks.

This isotopic shift therefore must be due to neutron capture and various decay modes of other trace impurities to ^{182}W or isobaric interferences. There are no impurities in the sample with high enough concentrations in which there would be an isobaric interference through another isotope with mass 182 or a polyatomic interference. It is believed that this increase in ^{182}W must be from irradiation of other trace impurities. Through further analysis, it was demonstrated that ^{181}Ta in the sample matrix is activated to ^{182}Ta which then beta decays to ^{182}W as can be seen in figure 4.5.

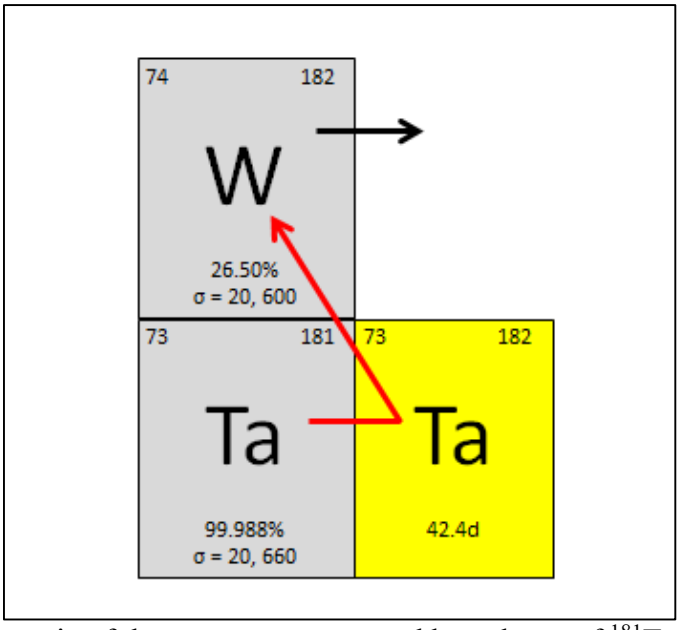

Figure 4.5: A schematic of the neutron capture and beta decay of ^{181}Ta to ^{182}W.

Under the same assumptions as used in the Pt calculations of a thermal neutron flux of $1x10^{14}$ and epithermal neutron flux of $1x10^{13}$, and the measured amount of Ta needed to produce ^{182}W, the amount of Ta needed to produce ^{182}W leading to the isotopic shift can be calculated as seen in table 4.23.

	Experimental	Bateman
[Ta] (ppm)	6170	911
Activity (Ci)	3	4.5

Table 4.23: The experimental and calculated concentration and activities of Ta in QSA source #38946239.

Based upon the ICP-QMS measured concentration of W of ~180ppm the estimated concentration of Ta in the iridium sample needed to double the amount of ^{182}W is calculated with equation 4.3 to be 911ppm. In order to verify the possibility of Ta being present in high enough concentrations to produce the W isotopic shift, both ICP-QMS and gamma spectroscopy can be used to verify the amount of Ta present. The data for trace impurities in activated iridium disks given in tables 4.13 and 4.14 shows a significant amount of Ta in table 4.13 with a concentration of 6170 ppm in disk #38946239. The disk #8423798437 however has a much lower Ta concentration of 162 ppm. This is consistent with the increase in the $^{182}W/^{184}W$ shift in disk #38946239 while there is a small change in the isotopic shift for disk #8423798437.

The presence of Ta can further be confirmed with gamma spectroscopy. Tantalum has a half-life of 42.4 days meaning that there will be quantifiable amount of ^{182}Ta present in the activated disk up to several years after irradiation. The activated disk #38946239 was measured with gamma spectroscopy with a high purity germanium detector in order to measure the activity of the ^{192}Ir, ^{194}Ir, and ^{182}Ta isotopes. Six years after the irradiation of the material there was ~3μCi of activity of Ta. Calculating the amount of activity of ^{182}Ta expected to be remaining after the decay time was calculated to be 4.5μCi.

An exact solution to the amount of ^{182}W produced can be calculated in the same manner as ^{195}Pt and ^{196}Pt with a solution to the Bateman equation which is given in equation 4.11.

$$N_{182W} = \Lambda_{181Ta}\Lambda^{*}_{182Ta}N^{0}_{181Ta}\left[\frac{e^{-\Lambda_{181Ta}t}}{(\Lambda_{182Ta}-\Lambda_{181Ta})(\Lambda_{182W}-\Lambda_{181Ta})}\right.$$

$$+\frac{e^{-\Lambda_{182Ta}t}}{(\Lambda_{181Ta}-\Lambda_{182Ta})(\Lambda_{182W}-\Lambda_{182Ta})}$$

$$\left.+\frac{e^{-\Lambda_{182W}t}}{(\Lambda_{181Ta}-\Lambda_{182W})(\Lambda_{182Ta}-\Lambda_{182W})}\right]$$

Equation 4.8: The exact solution of the Bateman equation for the production of ^{182}W from ^{181}Ta.

As can be seen in table 4.26 the presence of Ta in large enough amounts can produce the isotopic shifts seen in the experimental data. Using solutions to the Bateman equations the isotopic shift appears to be about an order of magnitude greater than the measured isotopic shift. Table 4.25 above shows the calculated concentration of Ta needed in the sample to produce the amount of isotopic shift measured at 911ppm and the actual measured concentration at 6170 ppm Ta. This explains the difference in the calculated isotopic shift and the experimentally measured one. Further work is being done to explain this discrepancy.

Identified Characteristics 4.6

A variety of natural, enriched, and activated iridium samples were analyzed. Various potential elemental and isotopic changes were identified in the samples.

Type of Source

Iridium sources can have multiple uses. They are produced most commonly for radiotherapy and radiography purposes. The first simplest method for identifying the type of source is through its physical shape and mass if it remained intact in the event.

Radiography sources are larger in disk shape at masses somewhere around 20 mg per disk. The medical sources come in the shape of a seed and are at masses around 5 mg. A second way to identify the type of source, especially if the source has been physically altered, is through the isotopic composition of the sample. Medical sources contain Ir which has been enriched to 80-85% ^{191}Ir while the radiography sources have much lower enrichment or are natural abundant Ir.

Origin of Source

Given the data collected, the presence or absence of a samples' trace impurities along with the concentrations of the impurities, samples from different locations can be differentiated. Iridium most commonly mined comes from various iron and copper sulfide ores which are thought to come from the same cosmic event [12]. Therefore, trace impurity differences in the samples are proposed to come from geochemical differences in the region of where the iridium was mined and processed. Variance in isotope ratios has also been used in nuclear forensic investigations for the identification of the origin of a material and where it was processed [8-10]. It is believed with this work that the sources can be discriminated by their trace-element concentrations.

Activation of Source

The activation of a source is done through neutron capture in a nuclear reactor. The fluence of a reactor can be identified through various isotope ratios. Isotopic ratios are influenced at predictable rates due to differences in neutron capture cross sections and the neutron environment. This work clearly demonstrates changes in the isotopic abundance of trace impurities in the source.

Age of Source

There are two different measurements that can be quantified with respect to the age of a source; the irradiation time and the time of decay since activation. The irradiation time can be estimated through isotopic shifts due to the burn-up rate of multiple isotopes. An isotope with larger cross section will absorb neutrons at a higher rate and become depleted with respect to isotopes with smaller cross sections. This will cause a shift in isotope ratios which can in turn be used to estimate the amount of time to cause such a shift.

With an estimation of the irradiation time, the activity of every isotope can also be estimated. With an estimate of the initial activity and the ability to perform gamma spectroscopy to determine the current activity of the same isotope, the amount of time for such decay can be determined.

Conclusions 4.7

Iridium samples including natural, enriched, and activated samples have all been dissolved electrochemically and analyzed with ICP-MS. The resulting data was used to develop trace elemental concentrations and isotope ratios which can be used for attribution of ^{192}Ir sources. Trace elemental signatures can used to help determine the origin of the iridium bulk material and potentially where it had been processed and sold. Isotopic signatures can be used for the determination of irradiation conditions, irradiation time, and decay time.

Chapter 5

RDD Explosives Tagging and Tracking

Introduction 5.1

In the forensics world, one of the most important objectives is the ability to identify and track explosive materials [42-43]. Explosive materials, both homemade and mass produced, have been used in criminal activities in threats and attacks around the world. The need for appropriate labeling and tracking techniques is vital to the security of the country and the safety of our armed services. This chapter describes current and potential future methods of tagging and tracking explosives used in illegal activities.

Explosives 5.2

Explosives are materials that react quickly in a violent manner to produce an explosion [42]. Explosives have been used for 100's of years for a variety of purposes including mining, fireworks, gun powder, and in warfare [42]. With increased terrorist activities over the last couple decades, the use of homemade and improvised explosive devices has been an area of great concern. One manner in which law enforcement would greatly be aided in tracking dangerous and explosives material would be to have an effective methods for tagging and tracking the materials typically used in an attack [43-48]. This section explores type of explosives and devices used in attacks.

Common compounds used

There are a variety of different compounds that are used in explosive materials. Most explosives are organics composed of C, N, O, and H. These compounds typically contain increased levels of N and O in the form of nitrates (NO_3) in relation to other

organic compounds [42, 44-48]. There also needs to be a "fuel" which will be exhumed. These fuels are primarily composed of hydrocarbons. It is the high density and the presence of nitrates which allows for a rapid oxidation of the hydrocarbons in the materials leading to the rapid exothermic reaction necessary for an explosive blast. These complex molecules break down into CO_2, N_2, and H_2O.

There are both traditional and non-traditional explosive materials which could potentially need tracking. Traditional explosives are chemicals made for the purpose of detonation for a variety of purposes such as mining, fireworks, and military purposes. Primary explosive materials are less common due to their instability and danger in transport and handling. Most common traditional explosives are considered secondary because they do not detonate readily with shock or heat. A list of some of the common explosives in each category are listed in table 5.1 [42, 48].

Traditional	**Non-traditional**
2,4,6-trinitrotolulene (TNT)	Ammonium Nitrate and Fuel Oils (ANFO)
octahydro-1,3,5,7-tetranitro-1,3,5,7-tetrazocine (HMX)	3,3-Dimethyl-1,2-dioxacyclopropane (Acetone Peroxide)
Penta-erythritol tetra-nitrate (PETN)	Urea nitrate
nitrocellulose	Jet fuel

Table 5.1: Common traditional and non-traditional explosives used for a variety of purposes.

Non-traditional explosives are materials which do not use common explosive compositions but rather are home-made with everyday chemicals. These differ from traditional explosives in that they are used for IEDs (Improvised explosive devices), home-made devices (HMDs), slurry explosives, liquid explosives, plastic-bonded explosives (PBXs), emulsion explosives, or "green" explosives [42, 48]. There are many

precursor chemicals that are used in non-traditional explosives. These every day chemicals include; acetone, ammonia, benzene, butane, ether, ethylene glycol, glycerin, iodine, lead, mercury, methane, nitric acid, perchloric acid, peroxide, silver, sulfuric acid, toluene, and urea [49]. A well know example of these compounds being used include the Oklahoma City bombing in which ANFO was used as the detonation material made from ammonium nitrate (fertilizer) and diesel fuel for the primary chemicals.

Types of devices

There are different types of devices used in attacks with IED's. These devices include; time-delayed, victim-operated, command-operated, and suicide bombers. Time-delayed devices are the more traditional type of devices where the system may be as simple as lighting a fuse to give the bomber time to retreat before detonation. Victim-operated improvised explosive devices (VOIED's) are devices which are activated by the victim through pressure sensors [48].

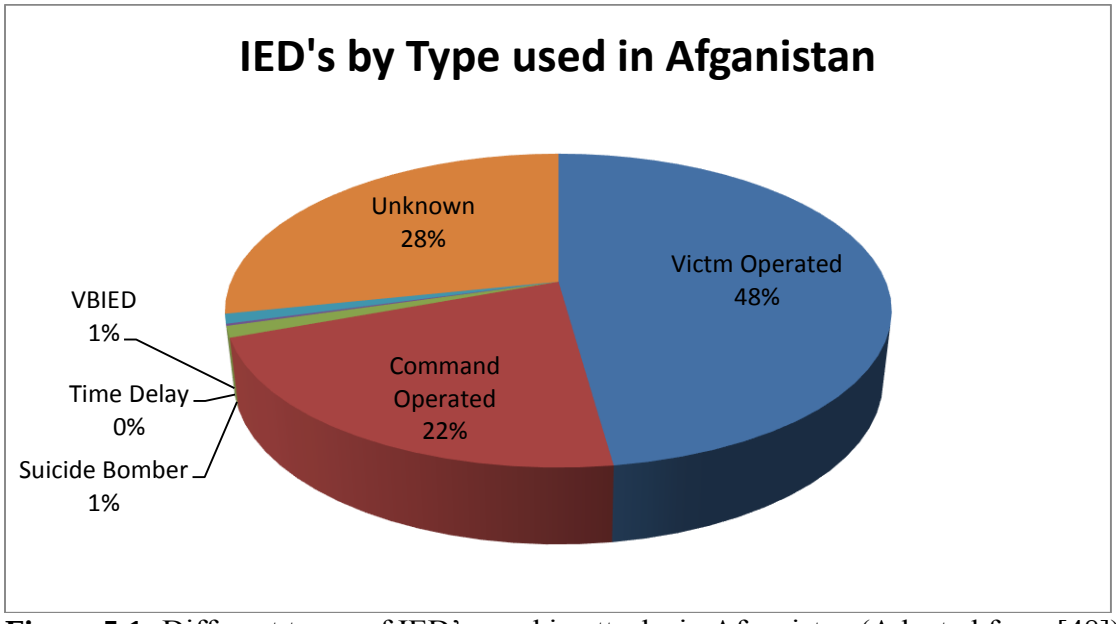

Figure 5.1: Different types of IED's used in attacks in Afganistan (Adapted from [48])

These type of devices include mail bombs and land mines. Command operated improvised explosive devices (COIED's) are devices which can be detonated from a distance. Typical COIED devices use electronics like cell phones, two way radios, or garage door openers to send a signal which detonates the device miles away from the device itself. The last form of device is operated by a suicide bomber. In this case an explosive device is strapped to a person who then uses some sort of switch or fuse to detonate the device killing or damaging people and property near the device including themselves. (Small Arms Survey) Figure 5.1 provides information on the types of devices used in attacks in Afganistan by terrorist groups. VOIED's and COIED's are by far the most used methods of attacks with IED materials. As can be seen, in the cases where the type of device could be identified, most are either victim operated (landmines) or command operated (cell phone activated). There are a significant number which could ultimately not be identified.

Methods of forensic analysis 5.3

Forensic investigation of attacks in which explosives were used is an important field especially in a post 9/11 world. While there is no consistent tagging and tracking method used for the identification of an explosive material and its origin, there are many techniques already used for analysis of explosives post detonation. Forensic analysis of a scene where detonation has occurred requires; characterization of the materials, a developed sampling method, and a method of detection [42]. The section below discusses various techniques currently used in forensic investigations.

Materials Characterization

There are a variety of methods for characterizing explosives materials. The number of methods of characterization has been expanding rapidly in recent years. There are surface adhesion methods which collect materials which have adhered to a surface such as a shoe, workbench, or hand where explosives have been worked with. Surface morphology of energetic materials is also important to help determine the detonation properties of an explosive substance. Various thermal excitation methods are used to identify explosives. This is possible because it has been shown that many explosives have vapor pressures and ignition points which are very sensitive to temperature [42]. There are many other techniques which have also been proposed or deployed involving terahertz responses and damage determination as well.

Sampling Method

There are a variety of methods used for the sampling of explosives. These methods include sampling of the gas phase chemicals, of the surface, and remote sensing of the bulk material. Sampling of gas phase chemicals requires a concentrating of the explosive gas phase residue using a sorption and then desorption process so the gas can be measured effectively. There are a variety of techniques used in the surface sampling of explosive samples. The most common of these was described above with swabbing of a surface and then counting of the swab to look for explosive residue.

Sample Detection

A variety of spectroscopic methods have been used in the detection of explosive compounds over the years. These methods include mass spectroscopy, ion mobility spectrometry, terahertz spectroscopy, infrared spectroscopy, laser induced spectroscopy, and various neutron activation analysis [42, 44-47]. Most methods of detection look for

molecular or atomic signatures which are unique to explosive and other energetic materials. In the case of mass spectroscopic or ion mobility analysis, molecular signatures which are unique to explosive materials are analyzed for the detection of materials. In the case of neutron activation the presence of high nitrogen and oxygen containing materials is scanned for.

Nanoparticles as taggants 5.4

There have been a variety of methods proposed to track dangerous or illicit materials. The fastest growing field in the chemical industry over the last 20 years is in nanochemistry and nanotechnology. Nano spheres, tubes, dots, and particles have been made through a variety of synthesis with different compositions from the light to the heavy elements [50-59]. Many different nanomaterials along with many different methods of analysis have been proposed for the tagging and tracking of materials and in particular explosives.

Tagging and tracking

The purpose of this investigation is to develop a barcode type system which can be used to track plastics such as various explosives, casing material on military weapons, chemicals that are used to produce explosives, etc. Tagging and tracking dangerous materials is important in forensic investigations which involve illegal activities of stealing, smuggling, and using dangerous materials in a terrorist attack. A barcode label can provide intelligence and law enforcement entities with information on the supplier, producer, manufacturer, and possibly even batch ID for the material used in attack. This valuable information can then be used to include or exclude potential suspects or theories about how the event occurred.

Various materials and analysis techniques have been proposed for the tagging and tracking of dangerous materials (explosives in particular). Methods of using taggant materials in explosives has been proposed and studied since the 1970's. In 1976 an advisory committee for the ATF developed and deployed a pilot program which used polymer micro-chip with unique magnetic and fluorescent properties [43]. The materials were deployed into multiple explosive materials from different companies and even used in the forensic investigation of a truck bombing in Baltimore in 1979. The program was later stopped due to evidence that the taggant had to be added at such high concentrations that it made the explosive material unstable and more highly reactive. The Office of Technology Assessment (OTA) was advised at the end of the program to evaluate the effectiveness of the taggant program. It was concluded that a taggant program would "probably retain substantial law enforcement utility" and "provide that increased utility in protecting those potential targets sufficiently important to warrant a detection taggant sensor" [43]. The study suggested that taggants could increase arrests related to bombings by as much as 75% [59]. While the assessment did note the potential usefulness of a taggant material, it did also acknowledge that implementation of such a program could increase costs of manufacturing by a great amount with as much as an order of magnitude of difference in the cost depending on the method implemented.

After the attack on a federal building in Oklahoma City in 1996, President Clinton pushed for the use of taggant materials for tracking explosive materials including explosives and gun powder. This attempt once again failed to make progress due to resistance from various political lobby groups (IME, NMA, and NRA) citing 2nd amendment and civil rights infringements, a lack of cost effective tagging and tracking

technique, and questions about the safety of adding taggant materials to explosives [59]. There is also added difficulty in tracking non-plastic explosives or chemicals where adding a taggant is more difficult [43].

There are many methods of tagging and tracking materials that have been proposed over the years. These methods utilize various physical and chemical properties including; magnetism, fluorescent, luminescent, calorimetric, optical absorption and emission, excitation, and nuclear properties. Proposed taggants include organic, metallic, and nanomaterials. Identified methods of analysis of these taggants include; Vapor/Particle Detection, Computed Tomography, Nuclear Quadrupole Resonance, Thermal Neutron Analysis, Electromagnetic Quadrupole Resonance, Nuclear Resonance Absorption, Pulsed Fast Neutron Radiography, Differential Scanning Calorimetry, Raman Scattering, and beyond. RFID tags have also been used in Australia for tracking explosives in the mining industry [49]. Most of the limitations relate to cost effectiveness, consumption during detonation, and effectiveness in identification due to matrix interferences.

Nanoparticles

Near the turn of the 20th to the 21st century the scientific world took a big turn with the discovery and rise of nanomaterials and nanoscience. Gold nanomaterials have been made since as early as the 4th century when unknown to its users it was being used to stain glass bowls and to make stained glass windows due to the unique red and blue tones it created [60]. This effect is now known to be due to the size that the gold nanoparticle is allowed to grow to. Nanomaterials are any structure whose size is on the order of 1 to 100 nanometers.

Nanosynthesis can be done in one, two or three dimensions in a variety of shapes including rods, spheres, tubes, sheets, and many more complex shapes. These materials can be self-assembling or be assembled through guided techniques. Nanomaterials have been made with metallic and non-metallic materials with C, Si, and the transition metals being some of the more commonly known nanomaterials. Research into the world of nanometer sized materials has had an impact all over the world. The field of materials science has been particularly affected by nanoscience with application in industries such as; semi-conductors, solar panels, make-up, sun block, clothing, etc. [60].

One field in which nanoparticles have been proposed to be utilized is for use as a taggant material for tracking dangerous or illicit materials. Many different types of nanodots or nanoparticles have been proposed as a taggant. One such proposal includes integration of multiple transition metal nanodots which have different melting points into an explosive material and using differential scanning calorimetry for analysis [58]. Another proposed method is to incorporate Cd/Te nanoparticles into the explosive material and analyze with INAA [52].

Lanthanide nanoparticles

Many published articles of the synthesis and analysis of lanthanide phosphate nanoparticles have been demonstrated for a variety of purposes because of their unique physical and chemical properties. These lanthanide phosphate nanoparticles were first developed for their unique ability to become luminescent. Potential applications for these nanoparticles include transparent sol–gel films that could have applications in light-emitting devices, lasers, optical or amplifiers [61-65] as well as targeted radiotherapy of cancer and other diseases [66-68]. An advantage outside of these uses is that lanthanides

have some of the largest thermal neutron cross sections of all the stable elements and relatively short half-lives making them ideal for NAA.

Nanoparticle Characterization

As discussed before, lanthanide phosphate nanoparticles have been synthesized and characterized previously by other groups. Previously published TEM images of $\{La_{0.5}Gd_{0.5}\}PO_4$ mixed cores have demonstrated that the size of $\{La_{0.5}Gd_{0.5}\}PO_4$ nanoparticle are typically 5 ± 1.5 nm in diameter. The particles appear to be semi-spherical in shape and close to uniform in size. XRD measurements also predict nanoparticles sizes of around 4-5 nm dependent upon the lanthanide composition as well. This suggests that the nanoparticle is in a single crystal form [68].

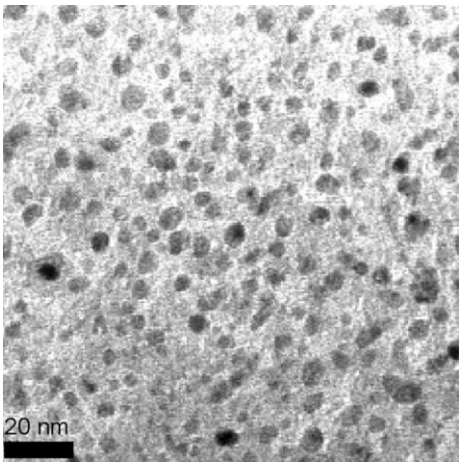

Figure 5.2: TEM image of $\{La_{0.5}Gd_{0.5}\}PO_4$ mixed core nanoparticles [68].

Magnetic separation techniques have also been used to confirm the mixed core composition of the nanoparticles. It has been demonstrated that in the presence of magnetic separation that La is retained along with Gd which suggests that the nanoparticles have mixed cores. Further imaging of the mixed core nanoparticles with electron energy loss spectroscopy (EELS) shows similar images for both the La and Gd

cameras. This is in agreement with magnetic separation techniques which suggest that the nanoparticles do have mixed cores of both La and Gd.

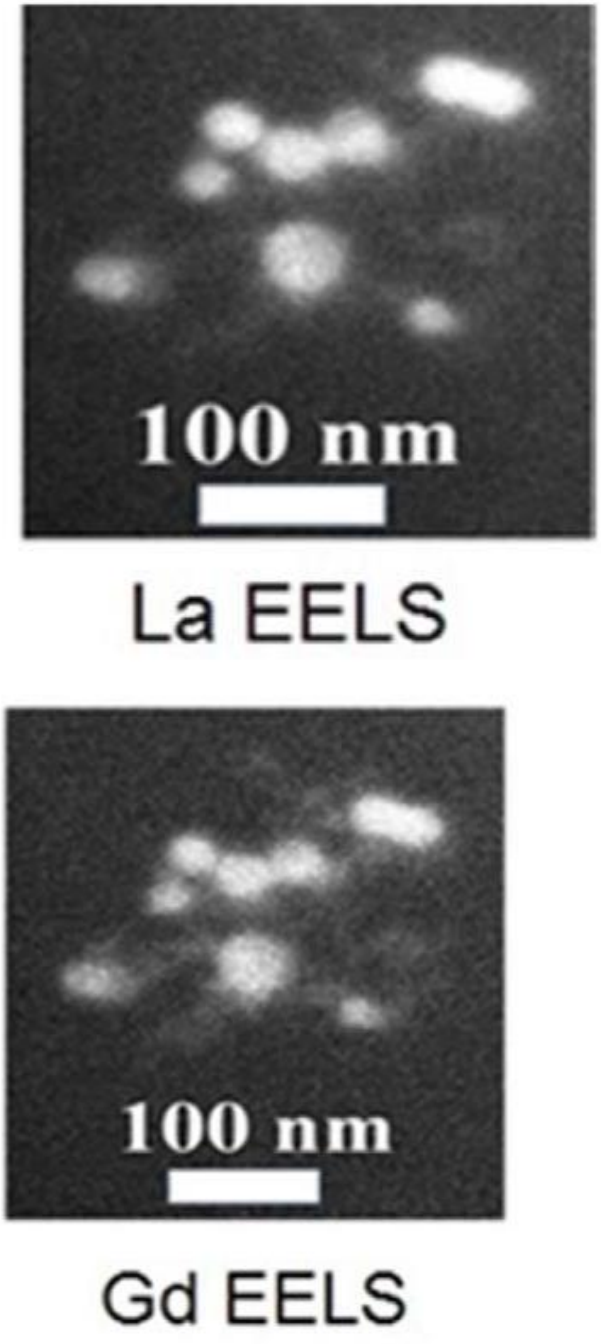

Figure 5.3: EELS images of Gd and La in mixed $\{La_{0.5}Gd_{0.5}\}PO_4$ nanoparticles [68].

Mixed core nanomaterials could be used as a useful taggant because they will retain their chemical signature through various chemical or physical changes. This is needed for effective taggants especially in a post-detonation scenario.

Lanthanide Taggants

Lanthanide phosphate nanoparticles (NP's) have been shown to be a stable material which retain their mixed core composition which is useful in tracer experiments [65-68]. The NP's also have a simple synthesis in aqueous solution making them easy to synthesize [61-65]. Therefore, these lanthanide phosphate nanoparticles could be of great use tracking many materials that are considered dangerous or of importance to the government. Possible lanthanides for use in tracking materials include; lanthanum, gadolinium, dysprosium, samarium, europium, and lutetium.

Isotope	Half-life ($T_{1/2}$)	Gamma E (keV)	Natural Isotopes	Nat. Ab. Stable Ln	Thermal σ (barns)
^{140}La	1.678 d	1596.2	^{139}La	99.910	9.39
^{165}Dy	1.26 m	515.5	^{164}Dy	28.260	2727.0
^{176}Lu	3.66 h	88.4	^{175}Lu	97.41	16.7
^{159}Gd	18.48 m	360.9	^{158}Gd	24.84	2.26
^{155}Sm	22.3m	104.33	^{154}Sm	22.75	103
^{152m}Eu	9.31h	841.57	^{151}Eu	47.81	1500

Table 5.2: Nuclear properties of selected elements to be used in $LnPO_4$ nanoparticles.

Nuclear properties of select isotopes from the lanthanide series are given in table 5.2. They show the favorable nuclear characteristics the lanthanides possess which makes them an appropriate choice for INAA. While NAA is an effective method for the characterization of most of the elements on the periodic table, using elements with the

largest of cross sections is necessary for analysis in the field. This is because NAA is typically done in the lab at a reactor where thermal neutron fluxes are on the order of 10^{14} $n*cm^{-2}*s^{-1}$ while hand portable neutron sources which could be used in the field have neutron fluxes around 10^{9} $n*cm^{-2}*s^{-1}$. This significantly lower neutron flux translates to a much slower activation rate of the irradiated sample. For fast, sensitive activation and analysis, the taggant material must have the most favorable neutron activation properties.

Another advantage of using the lanthanides as a material to track in the environment is their low abundance in the earth's crust. As can be seen in table 5.3 the lanthanides are all found at levels between 1 and 70 ppm with the majority falling below 10 ppm [69-70]. Using elements which are found in low abundances in the environment would provide a low background which would allow for lower detection limits for the nanoparticles if performing the analysis in the field. Keeping the nanoparticles at concentrations as low as possible is especially important as discussed before in order ensure that the nanoparticles do not affect the chemistry of the explosive material. The use of lanthanides as a taggant would then be one of the best materials for tracking with INAA.

	La	Ce	Pr	Nd	Pm	Sm	Eu	Gd	Tb	Dy	Ho	Er	Tm	Yb	Lu	Y
Crust (ppm)	35	66	9.1	40	0.0	7	2.1	6.1	1.2	4.5	1.3	3.5	0.5	3.1	0.8	31
Solar System (with respect to 10^{7} atoms Si)	4.5	1.2	1.7	8.5	0.0	2.5	1.0	3.3	0.6	3.9	0.9	2.5	0.4	2.4	0.4	40.0

Table 5.3: Abundances of the lanthanides in the earth's crust and solar system [70].

Instrumental Neutron Activation Analysis 2.5

Instrumental neutron activation analysis is a commonly used technique for the analysis of transition metals and lanthanides in sample masses of 10^{-6} to 10^{-12} grams [4].

NAA utilizes a (n,γ) reaction in which a neutron source is used to activate a sample matrix that is being investigated and the resulting activated nuclei are then measured by their emitted gamma rays via γ-spectroscopy as seen in figure 5.4. Activation analysis has many applications including the analysis of fine art objects, semi-conductors, forensic samples, rocks, minerals, water, and archeological samples. [4, 71]

Activation analysis involves the absorption of a neutron into a sample nucleus creating a compound nucleus. The compound nucleus then emits prompt and delayed gamma rays as well as beta particles at a consistent rate. The gamma rays of a radioactive nucleus are emitted at a specific energy which can then be measured to quantify the amount of an element in a sample. This process is shown schematically below in figure 5.4.

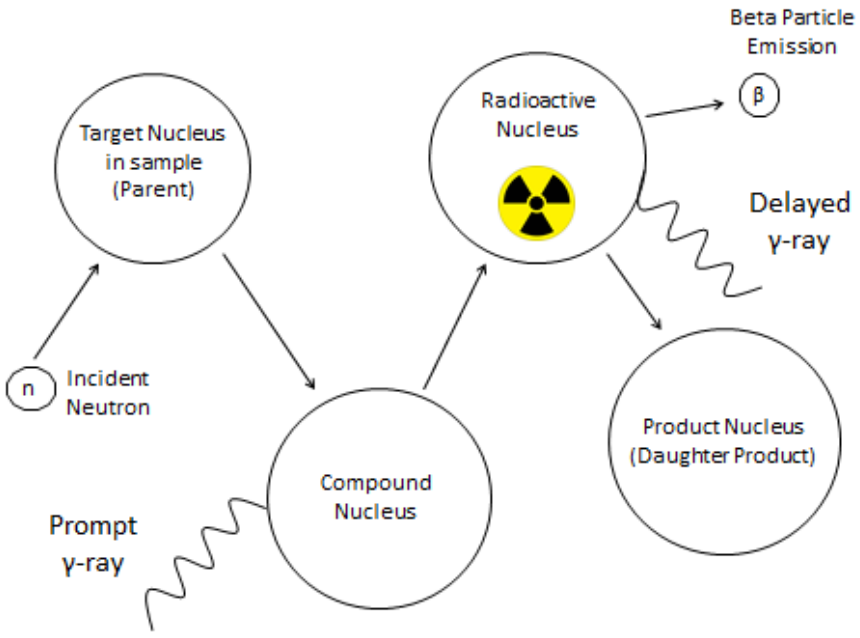

Figure 5.4: Scematic of the Neutron Activation Analysis (NAA) process of activation and decay of materials being investigated [72].

A few parameters govern the activation and decay processes involved in INAA. Equation 5.1 shows the aforementioned parameters that govern the activation of a material. The use of this equation shows larger cross sections, shorter decay times, and smaller half-lives produce higher levels of activity.

$$A = \sigma \Phi N_T (1 - e^{-\lambda \tau}) e^{-\lambda t}$$

A = Activity
σ=Cross section
Φ = Neutron flux
N_T = Number of atoms in target
λ = decay constant
τ = Irradiation time
t = Decay time

Equation: 5.1 The parameters that govern the activation of a material in a neutron rich environment.

The cross-section, often denoted with σ, is a parameter that provides the probability that a thermal neutron will absorb a neutron for a (n,γ) reaction. A common unit used for cross-sections are barns (b) which is equal to 10^{-24} cm^2. The flux, often denoted by Φ, is the number of neutrons that pass through a given area per unit time in the location in where irradiation and activation occurs. The flux is often given in units of $n*cm^{-2}*s^{-1}$ where, n= number of neutrons. Portable neutron sources often range in the $10^4 – 10^9$ $n*cm^{-2}*s^{-1}$ and reactors range in the $10^{13} – 10^{15}$ $n*cm^{-2}*s^{-1}$ [70-78].

There are many advantages for using NAA: its detection limits for transition metals and lanthanides are low, it is non-destructive, internal standards are not required, and measurements can be made in the field with a portable neutron source [76]. Another advantage that NAA holds over other methods of tagging materials is that investigative probe (the neutrons) as well as the measured signal (gamma rays) have very low

interaction with materials making sample matrix inference much less problematic. Because of these advantages NAA can be used for the tracking of nanoparticle barcode systems. NAA is particularly sensitive to lanthanide and transition metals due to the large cross sections of many of these elements, combined with the short half-lives of the produced daughters.

An additional advantage for the use of NAA is that portable sources (AmBe, PuBe, Cf^{252}, and Deuterium-Tritium generators [73-78]) can be used in the field for nondestructive analysis of materials. This provides the opportunity for fast detection and characterization of a potentially dangerous material. The lanthanide phosphate nanoparticles have the potential to be used by manufacturers and government agencies to label explosive materials for the ability to identify manufacturer information in the event of an explosive material being lost, stolen, or used in an attack.

MURR facilities

The University of Missouri Research Reactor has a 10MW light water reactor which uses HEU (Highly Enriched Uranium) for the fission of uranium as its neutron source. Samples for short irradiations are loaded into poly vials and then into poly "rabbits" for the pneumatic sample transport system. Rabbits with samples are shot through the pneumatic system and directly into the neutron rich environment of the reactor for irradiation. After irradiation the sample rabbit is sent back through the system into the laboratory where the samples are allowed to decay and then counted using gamma spectroscopy.

Gamma spectroscopy

Gamma spectroscopy is the most commonly used method for identifying radionuclides in the nuclear field. Scintillation (NaI) and semiconductor (HPGe's) detectors are the types of detection used in gamma spectroscopy. HPGe's are the detectors of choice for NAA because they have better resolution which is needed for complex samples and also produce lower detection limits. Each gamma ray which interacts with the Ge crystal produces an event which gets relayed to the counter. Each event is counted and placed into a bin based upon its energy. The resulting spectrum relays number of counts at each given energy. An example of a gamma spectrum is given in figure 5.5.

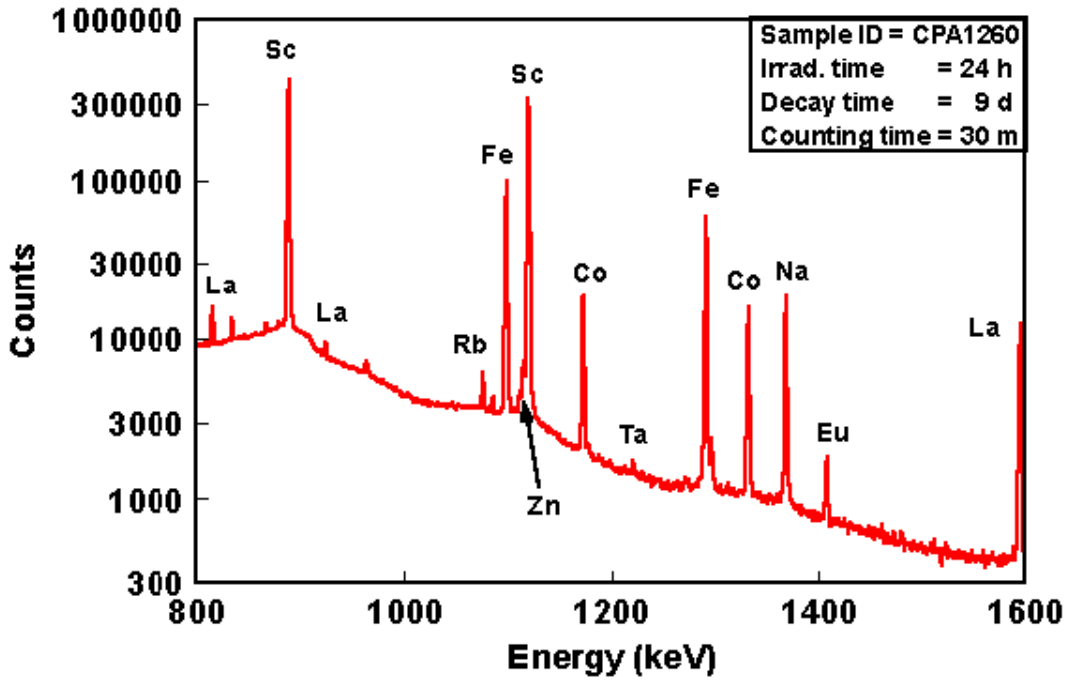

Figure 5.5: An example of a gamma spectra of an archaeometric sample [72].

Portable neutron sources

As shown above, in order to perform NAA, a neutron source is needed to activate that is material being interrogated. The fastest way to obtain information about a crime

scene requires that a rapid analysis is performed in the field. There are a variety of portable neutron sources which have been used for many years along with many newer sources which have been developed in recent years. The development of these sources makes in-field NAA possible. Portable neutron sources include, ^{252}Cf, D-D generators, and D-T generators.

Portable gamma spectrometers

In recent years with ever better electronics as well as semiconductors and cooling systems developments, gamma spectroscopy units are now being developed and sold in portable units. ORTEC is one such company which already has a line of HPGe instruments for sale to the general public as seen in figure 5.6.

Figure 5.6: Portable HPGe gamma spectroscopy unit sold by ORTEC.

The instrument is battery driven and light enough to be a handle held device. The system has an advanced cooling system which uses a mini Stirling-cycle cooler. This cooler

eliminates the need for liquid nitrogen cooling of the Ge crystal like most traditional detectors [79].

Conclusion 5.6

There is great need for the ability to tag and track materials used in improvised explosive devices used in illegal activities. Some reports estimate that the use of an effective taggant system could lead to as much as a 75% increase in the number of cases that are solved involving IED's. Lanthanide phosphate nanoparticles provide unique characteristics which make them ideal as a taggant material when tracked with INAA. Portable neutron source and gamma spectrometers could be used as means to identify the remains of the taggant in the field real time giving investigators and law enforcement fast accurate information as to where the material came from and how it was used.

Chapter 6

Method Lanthanide Nanoparticle Tracking with NAA

Introduction 6.1

Neutron Activation Analysis (NAA) is one of the most common radiometric techniques for the analysis and quantification of trace impurities in a sample. The lanthanides are some of the best samples to analyze with NAA because they have a large thermal neutron cross section. Therefore, the use of lanthanide phosphate nanoparticles as a tagging method with NAA as the method of detection provides the potential for a powerful method from tracking materials with lanthanide nanoparticles.

Nanoparticle Synthesis Method 6.2

A search of the literature shows, lanthanide phosphate nanoparticles have been synthesized, characterized, and discussed in detail [61-68]. The nanoparticles were synthesized by mixing a 1.5 mL of a 0.1M solution of sodium tripolyphosphate (TPP) with 1.5 mL of a 0.1M solution containing the desired molar ratio mixture of lanthanide salts in aqueous solution. All solutions were made with 18MΩ water. The solution was then mixed well until it turned clear. The solution was then heated at 90^{o} C for three hours. The resulting nanoparticles were visible in the bottom of the tube giving the solution a thick milky appearance. The nanoparticles were then separated from the ionic solution through dialyzing the nanoparticles in dialysis tubing of 6000-8000MW for 24-48 hours in an 18MΩ water bath. If the nanoparticles contained paramagnetic Gd, Dy, Eu, or Sm they were further separated through magnetic separation. The nanoparticles were set next to a 1 Tesla Nd magnet and allowed to sit for 24+ hours. The resulting

solution had all of the magnetic nanoparticles collected to the side with the magnet. Any remaining solution was pulled out with a pipet and the remaining nanoparticles were then re-suspended into solution.

Nanoparticle NAA Analysis Method 6.3

The composition and molar ratio of the lanthanides were confirmed by measuring an aliquot of the NP's with NAA at the University of Missouri's Research Reactor (MURR). Aliquots of 100µl (estimated to contain 10ug of lanthanides) of the nanoparticle solutions were pipetted onto filter paper inside ¼" dram vials. The total amount of the pipeted nanoparticle solution was measured gravimetrically. The samples were then capped and loaded into "rabbits" for irradiation. The samples were irradiated for 7 seconds, decayed for 60 seconds, and then were counted via gamma spectroscopy for 60 seconds. The net counts measured over the 60 second period are compared to counts measured of irradiated standards giving the amount of each lanthanide present in the nanoparticles. 10ug standards were prepared from standard solutions pipeted and measured gravimetrically. The standards were also capped, loaded into rabbits, and counted under the same conditions as the samples. Molar ratios and total mass of the nanoparticles were then calculated.

Gamma Spectroscopy Method 6.4

A gamma spectroscopy unit at MURR research facilities was used for the analysis of activated materials in the MURR research reactor. Samples were counted for 1 minute after a 1 minute decay. The samples were placed on a spinning sample holder 3 inches from the detector. The number of counts at a given energy for the sample were collected and a sample mass was determined using counts from external standards produced and

counted in the same manner as the samples. Final lanthanide masses were determined and the lanthanide ratios in the samples were then calculated.

Conclusions 6.5

Lanthanide phosphate nanoparticles varying in composition were synthesized in aqueous solution using a previously established method. Neutron activation analysis and was performed for the characterization of the synthesized lanthanide phosphate nanoparticles. The final lanthanide ratios were calculated to confirm the retention of the original lanthanide compositions.

Chapter 7

Nanoparticle Results & Discussion

Introduction 7.1

Lanthanide phosphate nanoparticles have been synthesized in aqueous solution varying in composition of the lanthanide as well as the ratios at which they are present. The nanoparticles were then quantified with NAA at the MURR reactor. The following results show the ability to make nanoparticles with mixed cores containing 1, 2, or 3 lanthanides and to be able to control the amount of each lanthanide in any given nanoparticle.

Two Lanthanide Nanoparticles 7.2

There are multiple publications over the past 15 years demonstrating the ability to synthesize mixed core lanthanide phosphate nanoparticles as well as lanthanide phosphate nanoparticles with differing lanthanide and transitions metal shells [58-68]. There has, however, been little work demonstrating the ability to vary the ratio of lanthanides contained in the core of this nanoparticle system [62].

Two Lanthanide Nanoparticle System

Experimental results for the synthesis of lanthanide phosphate nanoparticles which have been washed and magnetically separated demonstrated the ability to reliably synthesize mixed core nanoparticles containing two lanthanides at greatly varying molar ratios as seen in the following tables. Preliminary experiments containing nanoparticles with La:Gd, La:Dy, and La:Lu were synthesized in molar ratios from 90:10 to 10:90. The

data demonstrates the ability to synthesize La:Ln (where Ln = Dy, Lu) at a wide range of synthetic ratios.

Synthetic Ratio	La	Gd
La:Gd 40:60	45.7 ± 0.8	54.3 ± 0.8
La:Gd 50:50	50.9 ± 1.8	49.2 ± 1.8
La:Gd 90:10	93.2 ± 0.5	6.8 ± 0.5

Table 7.1: INAA data for the analysis of La:Gd nanoparticles at varying synthetic ratios.

Synthetic Ratio	La	Dy
La:Dy 40:60	38.4 ± 1.7	61.6 ± 1.7
La:Dy 60:40	65.7 ± 1.4	34.3 ± 1.4
La:Dy 90:10	93.8 ± 0.4	6.2 ± 0.4

Table 7.2: INAA data for the analysis of La:Dy nanoparticles at varying synthetic ratios.

Synthetic Ratio	La	Lu
La:Lu 70:30	79.4 ± 0.9	20.6 ± 0.9
La:Lu 90:10	97.0 ± 0.3	3.0 ± 0.3

Table 7.3: INAA data for the analysis of La:Lu nanoparticles at varying synthetic ratios.

As can be seen, the nanoparticles containing two lanthanides with close proximity (La:Gd) to one another and at extreme ends of the lanthanide series (La:Lu) can be synthesized. It was also demonstrated that the synthetic ratio could be varied over a wide range and the final mixed core composition retains the initial ratio.

Binary lanthanide nanoparticles were also synthesized with cores containing lanthanides other than lanthanum. Lu:Gd mixed core nanoparticles and gadolinium core with lutetium shell nanoparticles were synthesized and analyzed with INAA. Analysis was performed of the nanoparticle solutions in triplicate both before and after magnetic separation. Any shift in the elemental abundances after magnetic separation would suggest that the system was mixed nanoparticle cores instead of a single nanoparticle composition. The results of the analysis are given in table 7.4.

Synthetic Ratio	Lu	Gd	STDEV
Lu:Gd 33:67	36.4	63.6	0.6
Lu:Gd 33:67	36.4	63.6	0.1
Lu:Gd 33:67	28.9	71.1	0.8
Lu:Gd 33:67	28.7	71.3	0.8
La@Gd 50:50	47.0	53.0	1.1
La@Gd 50:50	46.4	53.6	0.3
La@Gd 50:50	46.7	53.3	0.8
La@Gd 50:50	47.4	52.6	1.6

Table 7.4: INAA data for the analysis of Gd:Lu and Lu@Gd nanoparticles. (Box in white = before magnetic separation, Box in gray = after separation.)

The data demonstrates that after washing and magnetic separation that there is no significant change in the measured lanthanides nor any shift in the La:Ln ratio. This is strong evidence that the nanoparticles have mixed cores that are uniform in nature. It is worth noting that this may not mean that each individual nanoparticle is homogenous. There are many possible ways in which individual nanoparticles may appear in the form of a "raisin bun" where the primary lanthanide composes the majority of the particle while small areas of the nanoparticle is comprised of secondary and tertiary lanthanides.

Identification of barcodes

In order to make a barcode system it is important to identify what the minimum change in the composition of the Taggant must be in order to identify it as a unique signature. Figures 7.1 and 7.2 show the different samples and the error in the final analysis of the composition of the nanoparticles. As can be seen nanoparticles need to have at least 10-12% difference in composition in order to have no overlap within the error leading to potential false identification.

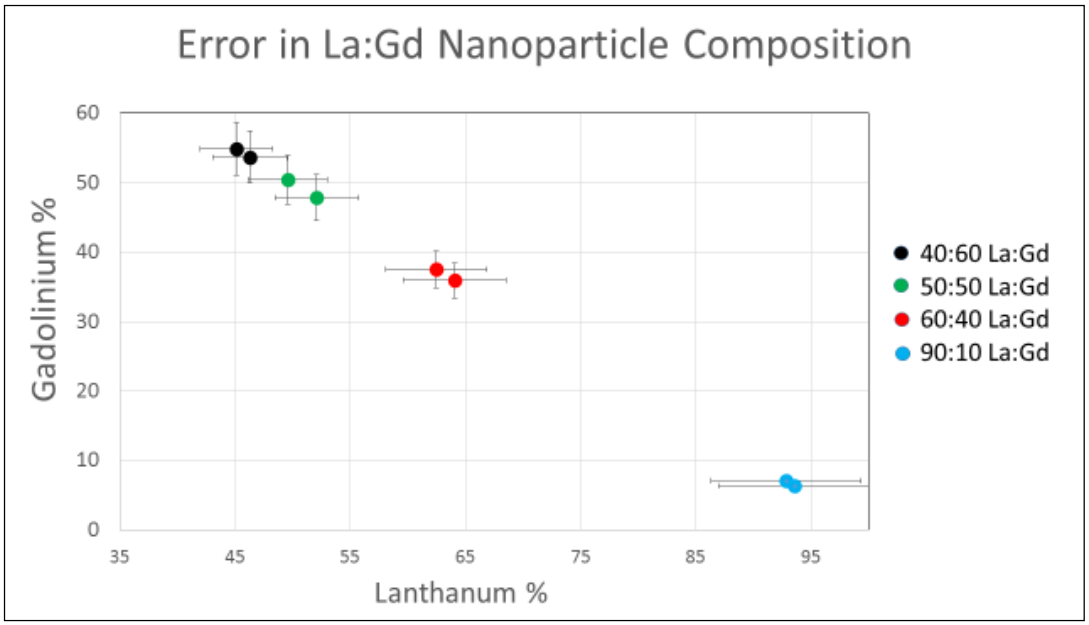

Figure 7.1: The measured elemental composition of La:Gd nanoparticles at different concentrations.

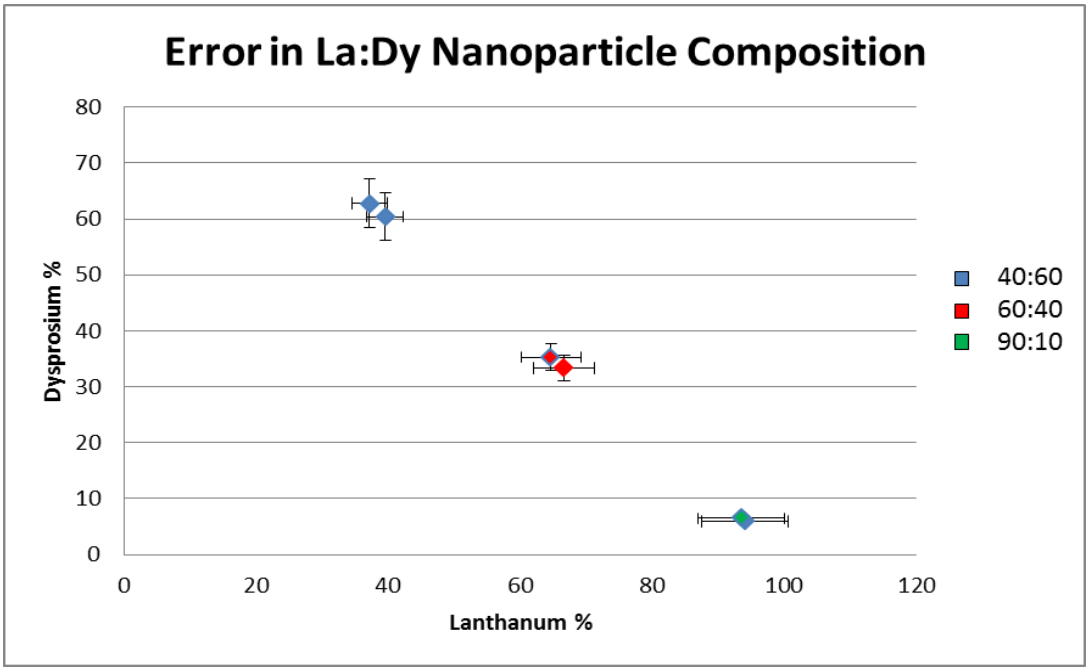

Figure 7.2: The measured elemental composition of La:Dy nanoparticles at different concentrations.

Trinary Lanthanide Nanoparticles 7.3

Once it was demonstrated that binary lanthanide phosphate nanoparticles could be synthesized over a wide range of lanthanides and composition, synthesis of trinary lanthanide phosphate mixed core nanoparticles were attempted. Data confirming the synthesis of the nanoparticle is given below.

The initial synthesis contained nanoparticles of La:Gd:Dy. The synthesis of any two of these three lanthanides in experiments shown in table 7.1 and 7.2 show that any binary combination of the three lanthanides is possible. Synthesis results of a trinary La:Gd:Dy nanoparticle is given in table 7.5.

Synthetic Ratio	La	Gd	Dy
La:Gd:Dy 80:10:10	39.7 ± 0.01	52.3 ± 0.04	8.1 ± 0.06
La:Gd:Dy 60:30:10	27.8 ± 0.2	63.0 ± 0.1	9.2 ± 0.1
La:Gd:Dy 60:20:20	18.1 ± 0.1	71.2 ± 0.1	10.7 ± 0.01
La:Gd:Dy 60:10:30	23.2 ± 0.4	66.2 ± 0.3	10.6 ± 0.1

Table 7.5: INAA data for the analysis of La:Gd:Dy nanoparticles at varying synthetic ratios.

As can be seen, the three lanthanide nanoparticles did not retain their synthetic ratio with the final solution containing a large shift in the Amount of Gd present, posing additional difficulties in creating a three lanthanide mixed core nanoparticle. Previous studies of lanthanide phosphate nanoparticles has demonstrated some interesting characteristics in the series of lanthanide phosphate nanoparticles. It has been previously published that lanthanides from La to Gd favor the formation of a rhabdophane crystal structure [62-64]. The lanthanides from Dy to Lu tend to from a monazite crystal structure [62-64]. The different crystal structures in the heavy and light lanthanides is attributed to the different ionic size of the lanthanides. This change in crystal structure is believed to be the source of increased Gd concentrations in the synthesized 3 lanthanide nanoparticle systems.

What is believed to have formed is a solution of La:Gd and Gd:Dy nanoparticles since Gd and Dy lie on opposite side of the lanthanide series. This is further supported by the fact that Gd lies on the edge of this transition and also is the lanthanide to increase its presence in the nanoparticle composition. At this point in time no published literature on La:Dy or La:Lu crystal structures is known to exist. According to Boakye and Mogilevsky, the mixture of Gd:Dy nanoparticles forms a xenomite crystal structure near room temperature while nanoparticles from La to Gd form a hexagonal rhabdophane crystal structure [62]. This information appears to follow the hypothesis that a mixture of La:Gd nanoparticles with a hexagonal rhabdophane crystal structure and Gd:Dy nanoparticles with a xenomite crystal structure have formed in the 3 lanthanide nanoparticle solution.

To test this hypothesis, and to find a potential three lanthanide mixed core nanoparticle which can be repeatedly synthesized without a shift from its synthetic ratio, the following was investigated. Mixed core trinary lanthanide nanoparticles using all lanthanides in the same region (light vs heavy) of the series were chosen and synthesized. The sythesis was performed with a mixture of Sm, Eu, and Gd. These were chosen because they all lie in the same region of the rhabdophane lanthanides and also are all adjacent to one another making them the most likely to form into a trinary lanthanide mixed core.

Synthetic Ratio	Gd	Sm	Eu
60:30:10	57.1 ± 0.7	33.8 ± 0.9	9.2 ± 0.1
60:20:20	61.2 ± 0.3	19.3 ± 2.1	19.6 ± 2.4
60:10:30	60.4 ± 0.3	12.7 ± 2.3	26.9 ± 2.7
80:10:10	80.0 ± 0.1	11.0 ± 0.1	9.0 ± 0.01

Table 7.6: INAA data for the analysis of Gd:Sm:Eu nanoparticles at varying synthetic ratios.

As can be seen in table 7.6 the newly synthesized nanoparticles formed at ratios similar to the original synthetic amounts. This suggests that the crystal structure is what is responsible for the problematic formation of the earlier three lanthanide series. In order to further confirm this, rather than synthesize a trinary lanthanide from elements immediately adjacent to one another, mixed core lanthanide particles were synthesized containing La:Gd:Sm or La:Gd:Eu covering the entire series of rhabdophane nanoparticles. The resulting data is given in table 7.7.

Synthetic Ratio	La	Gd	Sm	Eu
Gd:Sm:Eu 33:33:33	N/A	34.5 ± 0.7	34.9 ± 0.1	30.56 ± 0.6
La:Sm:Eu 33:33:33	35.0 ± 1.3	N/A	33.3 ± 0.9	31.1 ± 1.0
La:Sm:Eu 80:10:10	79.2 ± 1.8	N/A	10.6 ± 1.0	17.0 ± 0.7

Table 7.7: INAA data for the analysis of La:Gd:Sm and La:Gd:Eu nanoparticles at varying synthetic ratios.

As can be seen, the mixed core nanoparticles still form in the original synthetic ratios with no significant shift. With the provided information it is believed that mixed core three lanthanide nanoparticles can be synthesized at various synthetic ratios as long as the lanthanides of choice all form from the same crystalline structure.

Statistical Analysis 7.4

To make effective taggant, the nanoparticles must have a signature which must be clearly identifiable against other taggants. A statistical analysis of the measured values of different particles is needed to determine how much of a difference is needed for identification of a specific barcode.

One method of identifying groups of data (barcodes) within a series of samples based upon its composition with a high level of confidence is the provenance postulate. For many forms of materials studies the calculations or measurements made in an

investigation/study have been analyzed using the concept of the provenance postulate. This has been done to identify groups which have measured differences which are statistically significant from one another. The first formal definition was presented by in 1977 by Wiegand et al. [80-81], though there have been many others to also suggest its use. For the postulate to be valid and a sample to be differentiated, the data must meet the following conditions: the measured differences between sources must be greater than the measured differences within each of the given sources.

The provenance postulate can be applied to the composition of the nanoparticles data. As has been shown in the data table above and the figure 7.3 and 7.4 below, the composition of nanoparticles retains its original synthetic ratio within 10%. Therefore, according to the provenance postulate, if the composition of the nanoparticles varies the Ln:Ln or Ln:Ln:Ln ratios by more than 10% then, the nanoparticles barcodes can be identified as unique signatures and be differentiated from one another.

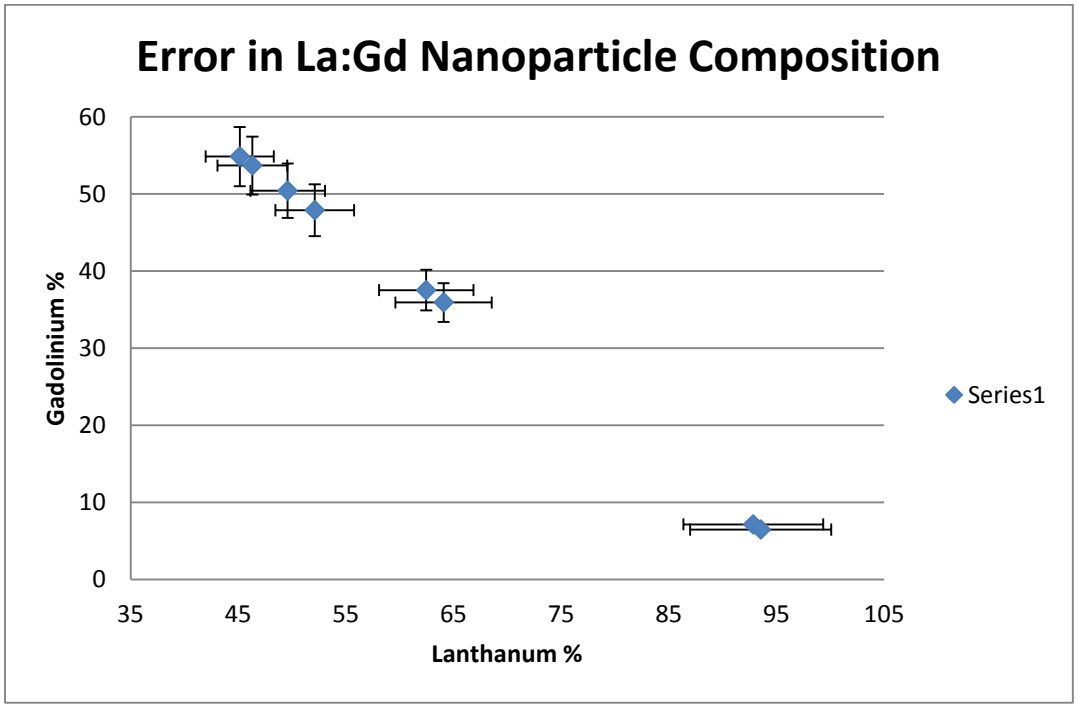

Table 7.3: The measured La:Gd ratio in varried nanoparticle samples.

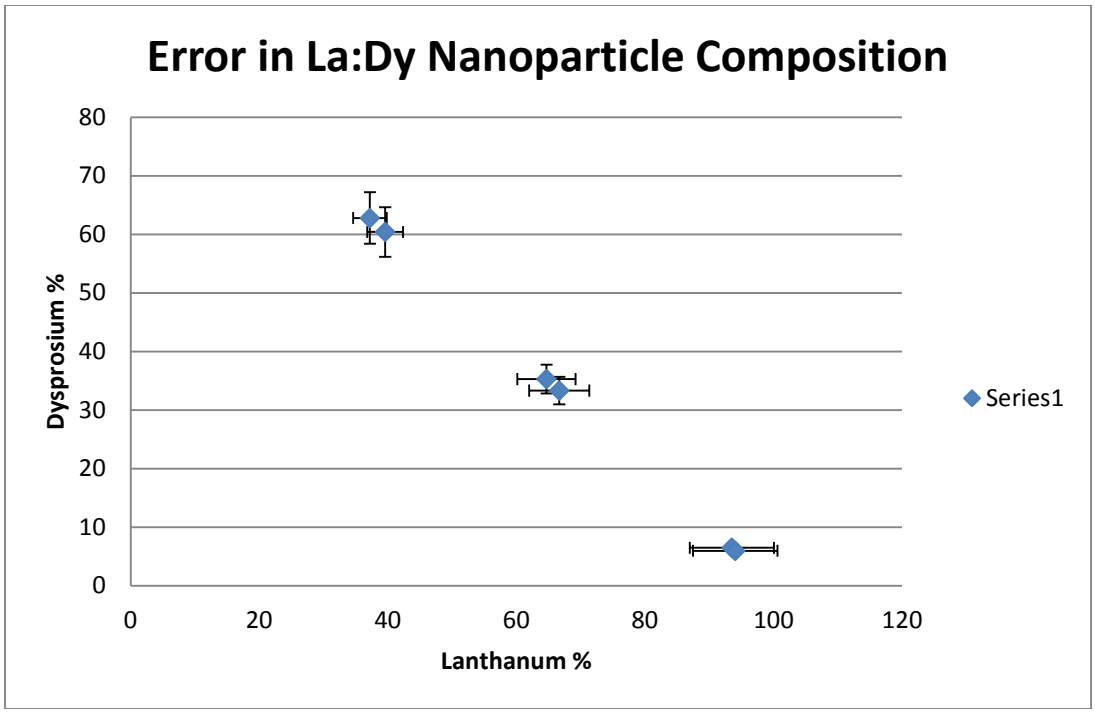

Table 7.4: The measured La:Gd ratio in varried nanoparticle samples.

Conclusions 7.5

Lanthanide phosphate nanoparticles have been synthesized containing two or three lanthanide mixed cores. The composition of the nanoparticles has been confirmed through various methods of washing and separation and analysis with INAA. Both the number of lanthanides and the molar ratio of the lanthanides were shown to retain the initial synthesized amounts added at the beginning of synthesis. One exception to the findings is that three lanthanide nanoparticles must contain lanthanides in similar groups within the lanthanide series due to changes in the crystal structure.

References:

1. Karam P. A., *Human and Ecological Risk Assessment* (HERA), **2005.**

2. Goldberg, M., Finck, M., *International Data on Radiological Sources.* INL/CON-10-18939 INMM 51**, 2010**.

3. Moody, K.J., Hutcheon, I.D., Grant, P.M. *Nuclear Forensic Analysis.* Taylor & Francis Group, **2005**, 2-15.

4. Loveland, W.D., Morrissey, D.J., Seaborg, G.T. *Modern Nuclear Chemistry.* Wiley & Sons Inc. **2006,** 366-372.

5. Loveland, W.D. *Basic Principles of Radiochemistry.* Radioanalytical Methods in Interdisciplinary Research; Laue, C., et al.; ACS Symposium Series; American Chemical Society: Washington, DC, **2003**.

6. Laue, C.E., Nash, K.L. *One Hundred Years of Development in Radioanalytical Chemistry as a Science to Probe the Limits.* Radioanalytical Methods in Interdisciplinary Research; Laue, C., et al.;ACS Symposium Series; American Chemical Society: Washington, DC, **2003**.

7. Stanley, F.E., Stalcup, A.M., Spitz, H.B. *A Brief Introduction to Analytical Methods in Nuclear Forensics.* Journal of Radioanalytical & Nuclear Chemistry, 295, **2013**, 1385-1393.

8. Krajko, J., Varga, Z., Yalcintas, E., Wallenius, M., Mayer, K. *Applications of Neodynium Isotope Ratio Measurements for the Origin Assesment of Uranium Ore Concentrates.* Tantala 129, **2014**, 499-504.

9. Sharp, N., McDonough, W.F., Ticknor, B.W., et al. *Rapid Analysis of Trinitie with Nuclear Forensic Applications for Post-Detonation Material Analyses.* Journal of Radioanalytical & Nuclear Chemistry. 302, **2014**, 57-67.

10. Lin, M., Zhao, Y., Li, L., et al. *Tracing Origins of Uranium Ore Concentrates (UCO's) by Multidimentional Statistics Analysis of Rare-Earth Impurities.* Journal of Analytical Atomic Spectometry, 0, **2014**, 1-8.

11. International Atomic Energy Agency. *Identification of Radioactive Sources and Devices.* IAEA **2007**.

12. Gill, R., *Modern analytical geochemistry: an introduction to quantitative chemical analysis for earth, environmental, and materials scientists*. Longman: Harlow, England, **1997**; p x, 329 p.
13. Taylor, L.; Papp, R. B.; Pollard, B. D., *Instrumental methods for determining elements*. VCH: New York, **1994**; p ix, 322 p.

14. Janssens, K.; Vittiglio, G.; Deraedt, I.; Aerts, A.; Vekemans, B.; Vincze, L.; Wei, F.; Deryck, I.; Schalm, O.; Adams, F.; Rindby, A.; Knochel, A.; Simionovici, A.; Snigirev, A., Use of microscopic XRF for non-destructive analysis in art and archaeometry. *X-Ray Spectrometry* **2000,** 29, (1), 73-91.

15. United States Geological Survey. *High Resolution ICP-MS Laboratory.* Retrieved: **4/2/2015** http://crustal.usgs.gov/laboratories/icpms/high_resolution.html

16. Perkin Elmer. *Manual of Perkin Elmer NEXION ICPMs 300S.* **2007**.

17. Argonne National Laboratory, EVS. *Iridium, Human Health Facts Sheet.* DOE, **2005**. Retrieved: March 2011 http://www.evs.anl.gov/pub/doc/Iridium.pdf

18. Williamson, J.F., Thomadsen, B.R., Nath, R. *Brachytherapy Physics.* Medical Physics Publishing: Madison, **1995**.

19. Van Tuyle, G. et al. *Reducing RDD Concerns to Large Radiological Source Applications.* Los Almaos National Laboratory, **2003**, 57.

20. Harris, D.C., Cabri, L.J. *Nomenclature of Platinum-Group-Element Alloys: Review and Revision.* Canadian Minerologist, 29, **1991**, 231-237.

21. Bernardis, F.L., Grant, R.A., Sherrington, D.C. *A Review of Methods of Spearation of the Platinum-Group Metals Through Their Chloro-Complexes.* Reactive & Functional Polymers, 65, **2005**, 205-217.

22. Seymore, R.J., O'Farrelly, J.I., *Platinum-Group Metals.* Kirk-Othmer Encyclopedia of Chemical Technology, John-Wiley & Sons: New York, **2000**.

23. Han, S.H., Varga, Z., Krajko, J. et al. *Measurement of the Sulfur Isotope Ratio $^{34}S/^{32}S$ Uranium Ore Concentrates (Yellow Cakes) for Origin Assessment.* Journal for Analytical Atomic Spectroscopy. 28, **2013**, 1919-1925.

24. Y-12 Online Site. *The Power to End a War: The History of the Calutron.* Retrieved **4/2/2015**. https://www.y12.doe.gov/sites/default/files/history/pdf/info_materials/05-0181.pdf

25. URENCO Online Site. *Urenco Stable Isotopes.* Retrieved: **4/2/2015** http://media.**urenco**.com/corp-website/74/stableisotopes_2.pdf

26. *Choppin, G.R., Lilgenzin, J.O., Rydberg, J. Radiochemistry and Nuclear Chemistry. Butterworth-Heinmann, **2002,** 393-396.*

27. *University of Missouri Archeometry. Overview of Neutron Activation Analysis. Retrieved 4/2/2015* http://archaeometry.missouri.edu/naa_overview.html

28. *Mayer, K., Wallenius, M., Varga, Z. Nuclear Forensic Science: Correlating Measureable Material Parameters to the History of Nuclear Material. Chemical Reviews,* ***2012****.*

29. Styrkas, A.D., Styrkas D. *Electrochemical Dissolution of Metals of the Platinum Group by Alternating Current.* Journal of Applied Electrochemistry. 25, **1995**, 440-494.

30. Saltykova, A.N., Baraboshkin, L.T., Kosikhin, S. *Salt Passivation During Anodic Iridium Dissolution in Chloride Melts.* Soviet Electrochemistry. 22 (5), **1986**, 545-550.

31. Box, W.D. ORNL-3802 (Gillete J.H., Editor) UC-23-Isotopes-Industrial Technology TID-450. 39th ed., **1964**, 26.

32. University of Missouri Research Reactor. *ICP-MS - Comparison of Techniques: Quadrupole.* Retrieved: 4/2/2015 http://www.murr.missouri.edu/ps_analytical_ICP_comparison_quadrupole.php

33. Glascock, M. D.; Braswell, G. E.; Cobean, R. H., *A systematic approach to obsidian source characterization.* Archaeological Obsidian Studies: Method and Theory, Shackley, M. S., Ed. Plenum Press: New York and London, **1998**, 15-65.

34. Baxter, M. J., *Exploratory multivariate analysis in archaeology*. Edinburgh University Press: Edinburgh, **1994**, 307

35. Parks, C.V. *Overview of ORIGEN2 and ORIGEN-S: Capabilities and Limitations.* Proceedings of the 1992 International High Level Radioactive Waste Management Conference, April 12-16, **1992** Las Vegas, NV.

36. Choppin, G.R., Liljenzin, J.O., and Rydberg, J. *Production of Radionuclides.* Radiochemistry and Nuclear Chemistry 3rd ed., Academic Press. **2013**, 388-397.

37. Rubinson, W. *The Equations of Radioactive Transformation in a Neutron Flux.* The Journal of Chemical Physics. 17 (6), **1949**, 542-547.

38. Centar, J. *General Solution of Bateman Equations for Nuclear Transmutations.* Annal of Nuclear Energy. 33, **2006**, 640-645.

39. Gold, L. *Method of Time-Free Solutions for Radioactive Decay and Radionuclide Production.* Journal of Applied Physics. 24 (1), **1953**, 88-90.

40. European-American Committee on Reactor Physics. *List of Research Reactors and Critical Facitilties.* International Atomic Energy Agency, **1974**.

41. Radiation Center-Oregon State University. *Research Reactors of the United States*. Nuclear Regulatory Commission. Retrieved: **4/3/2015** http://www.trtr.org/Res_Rx/facilities.html

42. Tourne, M. *Developments in Explosives Characterization and Detection.* Journal of Forensic Research, 12 (02), **2013**, 1-10.

43. Department of the Treasury. *Progress Report Study of: Marking, Rendering, and Liscencing of Explosives Materials.* Department of the Treasury, **1997**, 1-10.

44. Alfonso, K., Mashal, E., King, M., Strellis, D., Gozani, T. *MCNP Simulation Benchmarks for a Portable Inspection System for Narcotics, Explosives, and Nuclear Material Detection.* IEEE Transactions on Nuclear Science, 90 (2), **2013**, 520-527.

45. Allen, M., hertz, K., Kunz, C., and Mascarenhas, N. *A Portable Active Interrogation System Using a Switchable Neutron Source.* Proc. Of SPIE Vol. 5923, 592306 1-9.

46. Papp, A., Csikai, J. *Detection and identification of Explosives and Illicit Drugs Using Neutron Based Techniques.* J. Radioanal. Chem. 288, **2011**, 363-371.

47. Nasraradi, M.N., Bakhshi, F., Jalali, M., and Mahammadi, A. *Development of a Technique Using MCNPX Code for Determination of Nitrogen Content of Explosive Materials Using Prompt Gamma Neutron Activation Analysis Method.* Nuclear Instruments and Method in Physics Research A, 659, **2011**, 378-382.

48. Binnie, J., Wright, J. *'Infernal Machines' Explosive Devices.* Small arms Survey. **2013**, 220-246.

49. Rostberg, J.I. *Thesis: Common Chemicals as Precursers of Improvised Explosive Devices: The Challenges of Defeating Terrorism.* Naval Postgraduate School, **2015**.

50. Darnbrough, J. *Explosive Tracking System.* Mining Australia, **2008**, http://www.miningaustralia.com.au/news/explosive-tracking-system

51. National Nanotechnology Initiative. DTRA. Retrieved: **4/3/2015**, from http://www.nano.gov/node/849

52. Brown, S.S., Rondinone, A.J., and Dai, S. *Applications of Nanoparticles in Scintillation Detectors.* American Chemical Society Symposium: Washington D.C. **2007**.

53. Oak Ridge National Laboratory Review. *National Security Technologies: Preparing for the threats.* Oak Ridge National Laboratory. 39 (1), **2006**, 1-32.

54. Strem Nanoparticles. *Strem Nanomaterials for Defense & Security.* Strem Chemicals, INC. Retrieved: **4/3/2015**, http://www.strem.com/resource/5/25/strem_nanomaterials_for_defense_security

55. McNeil, S.E., United States Patent Application Pub. No.: US 2010/0304491Al, **2010**.

56. Service, R.F. *NRC Panel Enters the Fight Over Tagging Explosives.* Science, 275, **2007**, 474-475.

57. Gibbons, J.H. *Taggants in Explosives.* Congress of the United States Technology Assessment, **1980**.

58. Duong, B., Liu, H., Ma, L., & Su, M. *Covert Thermal Barcodes Based on Phase Change Nanoparticles*. Scientific Reports, 4 (5170), **2014**, 1-5.

59. Meyer, J., Feldman, P. *Oklahoma City: After the Bomb.* Los Angeles Times. **4/28/1995**.

60. Nano Text

61. Buissette, V., Moreau, M., Gacoin, T., Boilot, J.-P., Chane-Ching, J.-Y., and Le Mercier, T. *Colloidal Synthesis of Luminescent Rhabdophane LaPO:Ln*nHO (Ln = Ce, Tb, Eu;*0.7)Nanocrystals.* Chem. Mater., 16 (19), **2004**, 3767-3773.

62. Boakye, E.E., Mogilevsky, P., Hay, R.S., Fair, G.E. *Synthesis and Phase Composition of Lanthanide Phosphate Nanoparticles $LnPO_4$ (Ln= La, Gd, Tb, Dy, Y) and Solid Solutions for Fiber Coatings.* J. am. Ceramic Soc., 91 (12), **2008**, 3841-3849.

63. Buissette, B., Giaume, D., Gacoin, T., and Boilot, J.-P. *Luminescent Core/Shell Nanoparticles with a Rhabdophane $LnPO_4$-xH_2OStructure: Stabilization of Ce^{3+} - Doped Compositions.* Adv. Func. Mater. 16, **2006**, 351-355.

64. Meyssamy, H., Riwotzki, K., Kornowski, A., Naused, S., and Haase, M. *Wet-Chemical Synthesis of Doped Colloidal Nanomaterials: Particles and Fibers of $LaPO_4$:Eu, $LaPO_4$:Ce, and $LaPO_4$:Ce,Tb.* Adv. Mater. 1999, **11,** 840-844.

65. Buissette, V., Giaume, D., Gacoin, T., and Boilot, J.P. *Aqueous routes to lanthanide-doped oxide nanophosphors.* Journal of Materials Chemistry, 16, **2006**, 529-539.

66. Woodward, J., Kennel, S.J., Stuckey, A., Osborne, D., Wall, D., Rondinone, A.J., Standaert, R.F., and Mirzadeh, S. *LaPO4 Nanoparticles Doped with Actinium-225 that Partially Sequester Daughter Radionuclides.* Bioconjugate Chemistry, 22, **2011**, 766-776.

67. McLaughlin, M.F., Woodward, J., Boll, R.A., Wall, J.S., Rondinone, A.J., Mirzadeh, S., and Robertson, J.D. *Gold-Coated Lanthanide Phosphate Nanoparticles for an ^{225}Ac In-Vivo Alpha Generator.* Radiochimica Acta, 101, **2013**, 595-600.

68. McLaughlin, M.F., Woodward, J., Boll, R.A., Rondinone, A.J., Kennel, S.J., Mirzadeh, S., and Robertson, J.D. *Gold Coated Lanthanide Phosphate Nanoparticles for targeted Alpha Generator Therapy.* PLOS ONE, 8 (1), 2013, 1-8.

69. U.S. Geological Survey. *Rare Earth Elements—Critical Resources for High Technology*. Retrieved from at: http://geopubs.wr.usgs.gov/fact-sheet/fs087-02/

70. Cotton, S. *Lanthanide and Actinide Chemistry.* 2006. Wiley & sons Ltd.

71. Skoog, D.A., Holler, F.J., Crouch, S.R. *Radiochemical Methods.* Principles of Instrumental Analysis, Thompson Books/Cole; Belmont, CA, **2007**, 916-919.

72. Glascock, M.D. *Overview of Neutron Activation analysis*. University of Missouri Archaeometry Laboratory, **2012**, Retrieved: 4/3/2015 http://archaeometry.missouri.edu/naa_overview.html

73. Allen, M., Hertz, K., Kunz, C., Mascarenhas, N. *A Portable Active Interrogation System Using a Switchable AmBe Neutron Source.* Proc. Of SPIE, 5923 (592306), **2005**, 1-9.

74. Christian, J.F., Sia, R., Dokhale, P., Shestakova, I., Nagarcar, V., et al. *Nuclear Material Detection Techniques.* Proc. Of SPIE, 6945 (69451Q), **2008**, 1-9.

75. The Working Group on Nuclear Techniques in Hydrology. *Nuclear Well Logging in Hydrology.* International Atomic Energy Agency, 126, **1971**, 9-16.

76. Katalenich, J., Flaska, M., Pozzi, S.A., Hartman, M.R. *High-Fidelity MCNP Modeling of a D–T Neutron Generator for Active Interrogation of Special Nuclear Material.* Nuclear Instruments and Methods in Physics Research A, 652, **2011**, 120-123.

77. Nasrabadi, M.N., Bakhshi, F., Jalali, M., Mohammadi, A. *Development of a Technique Using MCNPX Code for Determination of Nitrogen Content of Explosive Materials Using Prompt Gamma Neutron Activation Analysis Method.* Nuclear Instruments and Methods in Physics Research A, 659, **2011**, 378-382.

78. Ellsworth, J.L., Tanga, V., Falabella, S., Naranjo, B., and Putterman, S. *Neutron Production Using A Pyroelectric Driven Target Coupled With A Gated Field Ionization Source.* Application of Accelerators in Research Industry, 1525, **2013**, 128.

79. Direct Industry. *Portable Gamma Spectrometer.* Ortec, Retrieved **4/3/2015** http://www.directindustry.com/prod/ortec/gamma-spectrometer-portable-laboratory-usb-50423-430219.html#product-item_430232

80. Weigand, P. C.; Harbottle, G.; Sayre, E. V., *Turquoise Sources and Source Analysis: Mesoamerica and the Southwestern U.S.A.* Academic Press: New York, **1977**.

81. Wilson, L.; Pollard, A. M., *The Provenance Hypothesis. In Handbook of Archaeological Sciences*, Brothwell, D. R.; Pollard, A. M., Eds. John Wiley and Sons, Ltd.: Chichester, **2001**, 507-517.

Appendix: A

Chemical Separations of Iridium

Purification Methods

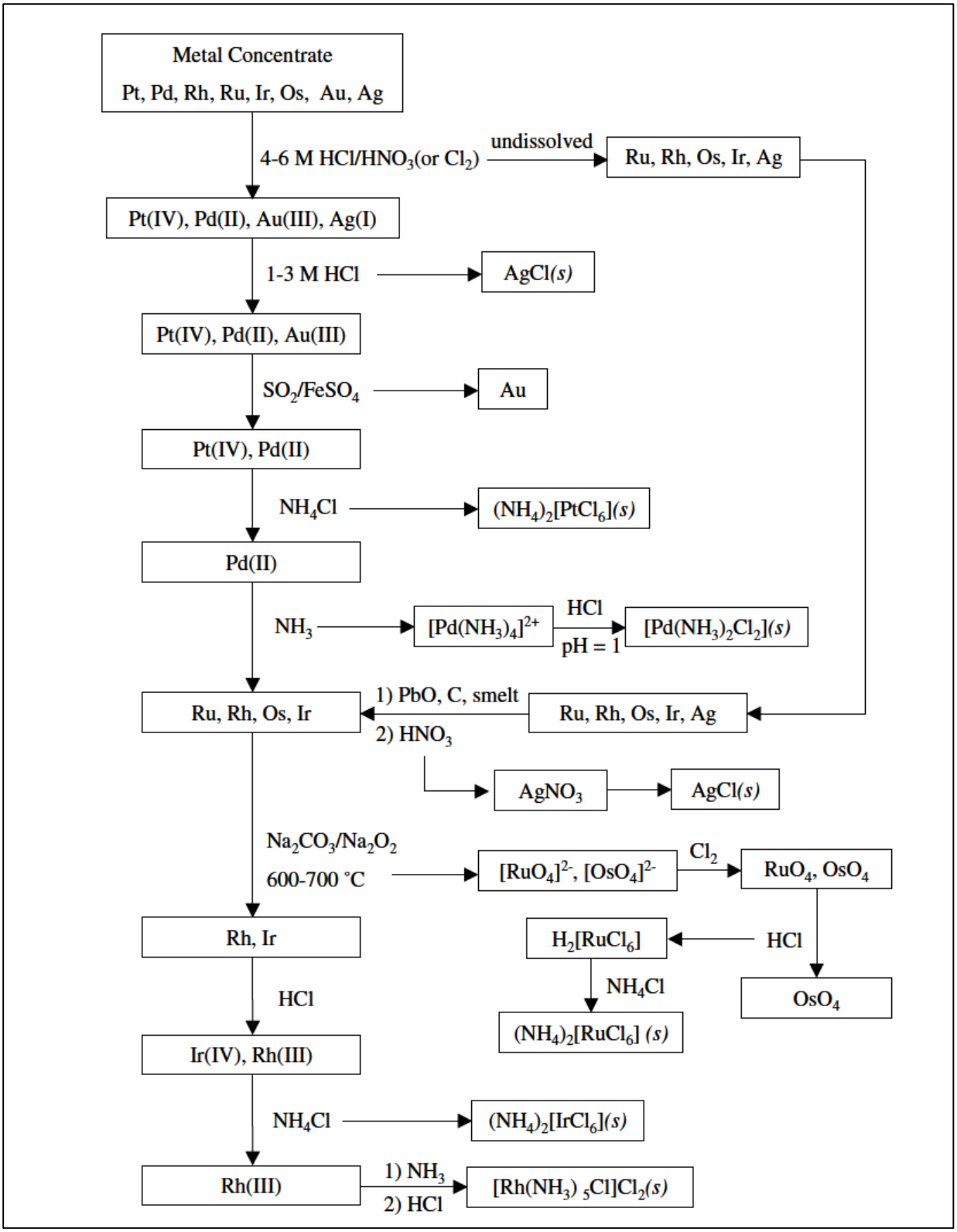

Figure 2.4: Classical (organic phase) method for the refining separation method of PGM's [21].

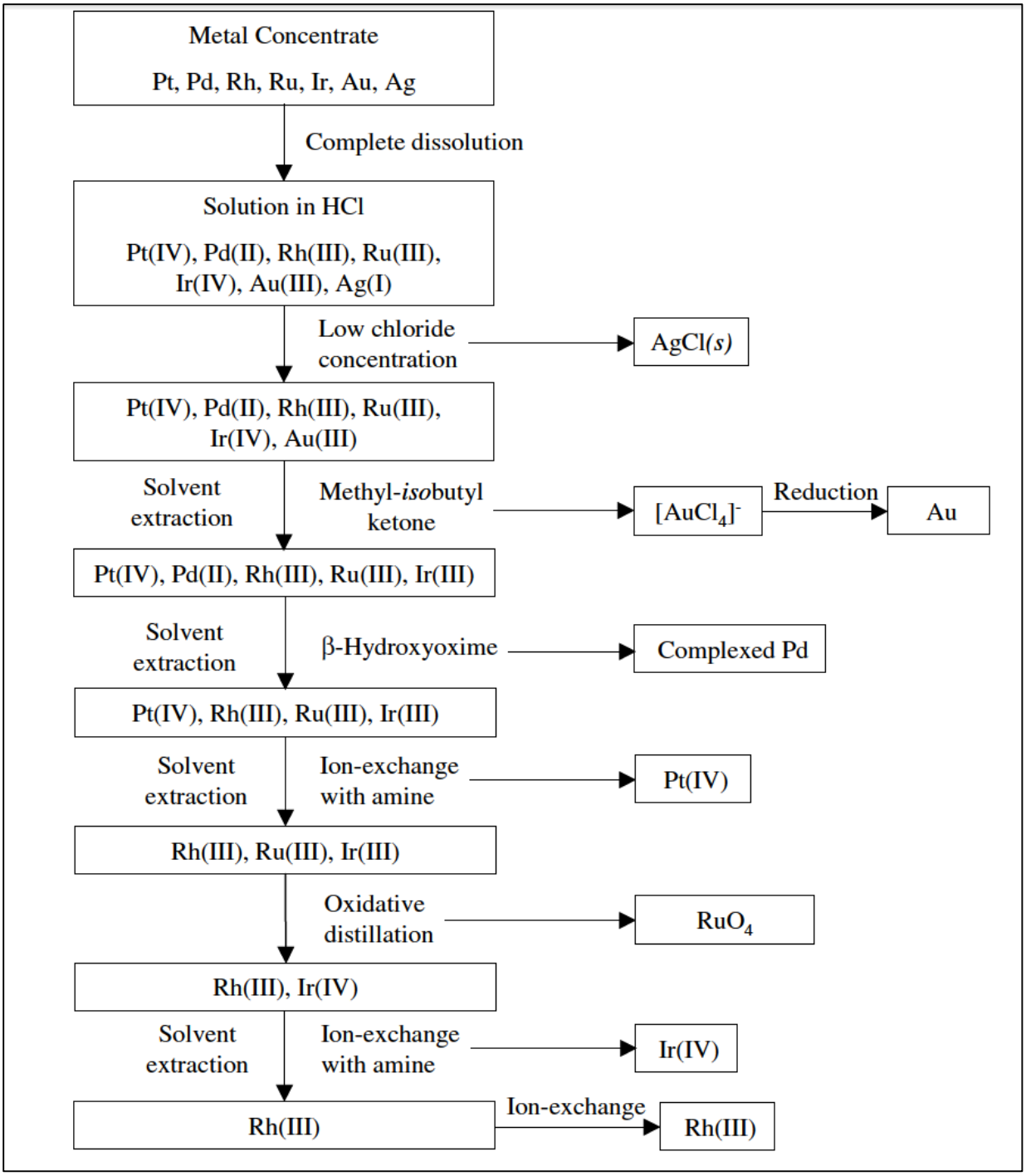

Figure 2.5: Modern refining method using solvent extraction/ion exchange [21].

Appendix: B

ICP-MS Reagents and Standards

ICP-MS-B Multi-Element Standard 10ug/mL in 10% HCl

Ce	Dy	Er	Eu	Gd	Ho	La	Lu	Nd	Pr	Sc	Sm	Tb	Th	Tm
Y	Yb													

ICP-MS-C Multi-Element Standard 10ug/mL in 2% HNO_3

Au	Hf	Ir	Pd	Pt	Rh	Ru	Sb	Sn	Te

ICP-MS-D Multi-Element Standard 10ug/mL in 2% HNO_3

B	Ge	Mo	Nb	P	Re	S	Si	Ta	Ti	W	Zr

MSCS-M Multi-Element Standard 10ug/mL in 2% HNO_3

Ag	Al	As	B	Ba	Be	Bi	Ca	Cd	Co	Cr	Cu	Eu	Fe	Ho
La	Li	Mg	Mn	Mo	Na	Ni	Pb	Sb	Se	Sr	Th	Tl	U	V
Yb	Zn													

ICP-MS Thallium Standard 1000ug/mL in 2% HNO_3

ICP-MS Cadmium Standard 1000ug/mL in 2% HNO_3

ICP-MS Scandium Standard 1000ug/mL in 2% HNO_3

ICP-MS Indium Standard 1000ug/mL in 2% HNO_3

VITA

Isaac Simmonds was born in Los Alamos, NM on August 31, 1987. He was homeschooled through high school and graduated in May of 2005. Isaac developed interests in radioanalytical chemistry with particular interests in nuclear forensics, isotope production, nuclear medicine and the greater nuclear and analytical chemistry science fields. Isaac received his bachelor's of science from New Mexico State University in Chemistry in December of 2009 also having internships under Dr. Gary Eicmen and at NMSU as well as with the health physics group at Los Alamos National Laboratory during his undergraduate studies. Isaac began graduate school at the University of Missouri in the fall of 2009. Isaac married his wife Krystal June 4, 2011 and has to sons Jaden (1 ½) and Luke (5 mo.). Isaac earned his doctorate in radiochemistry from MU May of 2015 and has begun a full time staff position as radiochemist at Northstar Medical Radioisotopes in Madison, WI.